JCB Journal of Cell Biology

ARTICLE

Centromere-localized Aurora B kinase is required for the fidelity of chromosome segregation

Cai Liang[1*], Zhenlei Zhang[1*], Qinfu Chen[1], Haiyan Yan[1], Miao Zhang[1], Linli Zhou[1], Junfen Xu[2], Weiguo Lu[2,3], and Fangwei Wang[1,2]

Aurora B kinase plays an essential role in chromosome bi-orientation, which is a prerequisite for equal segregation of chromosomes during mitosis. However, it remains largely unclear whether centromere-localized Aurora B is required for faithful chromosome segregation. Here we show that histone H3 Thr-3 phosphorylation (H3pT3) and H2A Thr-120 phosphorylation (H2ApT120) can independently recruit Aurora B. Disrupting H3pT3-mediated localization of Aurora B at the inner centromere impedes the decline in H2ApT120 during metaphase and causes H2ApT120-dependent accumulation of Aurora B at the kinetochore-proximal centromere. Consequently, silencing of the spindle assembly checkpoint (SAC) is delayed, whereas the fidelity of chromosome segregation is negligibly affected. Further eliminating an H2ApT120-dependent pool of Aurora B restores proper timing for SAC silencing but increases chromosome missegregation. Our data indicate that H2ApT120-mediated localization of Aurora B compensates for the loss of an H3pT3-dependent pool of Aurora B to correct improper kinetochore–microtubule attachments. This study provides important insights into how centromeric Aurora B regulates SAC and kinetochore attachment to microtubules to ensure error-free chromosome segregation.

Introduction

Faithful chromosome segregation during mitotic cell division requires that each pair of sister kinetochores binds to microtubules emanating from opposite spindle poles (bi-orientation). The kinetochore assembles at the centromere of each chromosome to mediate interactions with spindle microtubules (Cheeseman, 2014). Kinetochores also recruit proteins to regulate the spindle assembly checkpoint (SAC), a surveillance mechanism that monitors the status of kinetochore–microtubule (KT-MT) attachments and delays anaphase onset until all kinetochores are attached to microtubules (Musacchio, 2015). Kinetochores can be divided into two layers, where the constitutive centromere-associated network (CCAN) resides at the inner kinetochore and the Knl1/Mis12 complex/Ndc80 complex (KMN) network resides at the outer kinetochore (Musacchio and Desai, 2017). Within the KMN network, Knl1 is responsible for recruiting proteins that regulate SAC, the Mis12 complex anchors the network to the CCAN, and the Ndc80 complex binds to microtubules (Varma and Salmon, 2012).

Knl1 possesses a large disordered N-terminal region with multiple conserved motifs (Caldas and DeLuca, 2014). Residing at the far N-terminus is the protein phosphatase 1 (PP1)–binding site, termed SSILK and RVSF motifs (Hendrickx et al., 2009), following which there are multiple MELT motifs that are scattered along the N-terminal half of Knl1. In early mitosis, the SAC kinase Mps1 localizes to unattached kinetochores and phosphorylates the threonine residue in the Knl1-MELT repeats, which in turn recruits the SAC protein Bub3 together with Bub1 and BubR1 (collectively referred to as Bubs) to enable SAC activation (Krenn et al., 2014; London et al., 2012; Primorac et al., 2013; Shepperd et al., 2012; Vleugel et al., 2013, 2015; Yamagishi et al., 2012; Zhang et al., 2014). Meanwhile, Aurora B kinase phosphorylates the serine residue in the Knl1-RVSF motif to inhibit the Knl1–PP1γ interaction (Liu et al., 2010). Upon chromosome alignment on the metaphase spindle, dephosphorylation of the Knl1-RVSF motif results in the recruitment of PP1γ, which in turn dephosphorylates the MELT repeats to release Bubs, eventually leading to SAC silencing and mitotic exit (Espeut et al., 2012; London et al., 2012; Meadows et al., 2011; Nijenhuis et al., 2014; Pinsky et al., 2009; Rosenberg et al., 2011; Vanoosthuyse and Hardwick, 2009; Zhang et al., 2014).

Hec1 in the Ndc80 complex is important for the binding of kinetochores to microtubules (Monda and Cheeseman, 2018). In response to lowered tension across kinetochores, Aurora B

[1]MOE Laboratory of Biosystems Homeostasis and Protection and Innovation Center for Cell Signaling Network, Life Sciences Institute, Zhejiang University, Hangzhou, Zhejiang, China; [2]Department of Gynecological Oncology, Women's Hospital, Zhejiang University School of Medicine, Hangzhou, Zhejiang, China; [3]Women's Reproductive Health Key Research Laboratory of Zhejiang Province, Women's Hospital, Zhejiang University School of Medicine, Hangzhou, Zhejiang, China.

*C. Liang and Z. Zhang contributed equally to this paper; Correspondence to Fangwei Wang: fwwang@zju.edu.cn.

phosphorylates multiple serine/threonine residues within the N-terminal tail of Hec1 to destabilize microtubules that are improperly attached and to allow another chance for proper attachment to form (Cheeseman et al., 2006; Ciferri et al., 2005, 2008; DeLuca et al., 2006, 2011; Guimaraes et al., 2008; Miller et al., 2008; Welburn et al., 2010). This trial-and-error process is pivotal for the correction of aberrant KT-MT attachments (Hauf et al., 2003; Lampson et al., 2004). When chromosomes are aligned at the metaphase plate, these Aurora B target sites are dephosphorylated, resulting in stabilization of microtubule attachments. Thus, through phosphorylating the Knl1-RVSF motif and the N-terminal segment of Hec1, Aurora B plays an essential role in chromosome bi-orientation.

Aurora B is the enzymatic component of the chromosomal passenger complex (CPC), which also includes the regulatory subunits Survivin, Borealin, and inner centromere protein (INCENP; Carmena et al., 2012). During prophase through metaphase, CPC predominantly localizes to the inner centromere, a specialized chromatin region that lies at the intersection of the interkinetochore axis and inter–sister chromatin axis. Localization of Aurora B at the inner centromere is central to the prevailing tension-based spatial separation model for how Aurora B senses and corrects erroneous KT-MT attachments (Lampson and Cheeseman, 2011; Liu et al., 2009; Tanaka et al., 2002). However, this view has been challenged by several surprising observations that inner-centromeric localization of Aurora B is dispensable for chromosome bi-orientation in budding yeast (Campbell and Desai, 2013), chicken cells (Yue et al., 2008), and human cells (Hengeveld et al., 2017). Whether and how centromere-localized Aurora B regulates chromosome bi-orientation and segregation remains a major outstanding question (Bekier et al., 2015; Campbell and Desai, 2013; De Antoni et al., 2012; Hindriksen et al., 2017; Knowlton et al., 2006; Krenn and Musacchio, 2015; Lampson and Cheeseman, 2011; Lan et al., 2004; Liu et al., 2009; Wang et al., 2012; Welburn et al., 2010; Yoo et al., 2018; Yue et al., 2008).

An intricate and evolutionarily conserved signaling network involving Haspin-mediated histone H3 Thr-3 phosphorylation (H3pT3) and Bub1-mediated histone H2A Thr-120 phosphorylation (H2ApT120) underlies the defined localization of Aurora B at the inner centromere. H3pT3 is concentrated at the inner centromere (Dai et al., 2005, 2006) and is directly recognized by Survivin (Kelly et al., 2010; Wang et al., 2010; Yamagishi et al., 2010). H2ApT120 is enriched at the KT-proximal centromere and is directly recognized by Sgo1 (Kawashima et al., 2010; Liu et al., 2015), which in turn recruits Cdk1-phosphorylated Borealin (Tsukahara et al., 2010). It has been proposed that CPC localization at centromeres requires the combination of these two histone marks (Yamagishi et al., 2010). However, the underlying molecular mechanism remains elusive (Krenn and Musacchio, 2015; Trivedi and Stukenberg, 2016; Hindriksen et al., 2017). Here we show how these two phospho-histone marks collaborate to control the localization and activity of Aurora B at centromeres to ensure the fidelity of chromosome segregation during mitosis.

Results

Either H3pT3 or H2ApT120 alone is sufficient to recruit Aurora B

To investigate how H3pT3 and H2ApT120 localize the CPC to inner centromeres, we first tested whether these two histone marks could recruit CPC independently, using a U2OS-derived cell line in which multiple copies of Lac Operator (LacO) repeats were stably integrated in an euchromatic region of chromosome 1 (Janicki et al., 2004). As expected, tethering EGFP-fused Lac repressor (EGFP-LacI) alone to the LacO array did not generate H3pT3 or H2ApT120 (Fig. 1, A–C). While tethering Haspin kinase domain as a fusion protein with EGFP-LacI (EGFP-LacI-Haspin-K) to the LacO array generated H3pT3 but not H2ApT120, tethering EGFP-LacI–fused Bub1 kinase domain (EGFP-LacI-Bub1-K) generated H2ApT120 but not H3pT3 in interphase cells. By contrast, the kinase-dead mutant forms of Haspin (K511A) and Bub1 (D946N) were unable to do so. Importantly, expression of EGFP-LacI-Haspin, but not EGFP-LacI or EGFP-LacI-Haspin-K511A, generated H3pT3 and recruited Aurora B (Fig. 1, D and E). Thus, H3pT3, presumably through binding Survivin, can recruit Aurora B to an ectopic chromatin locus in the absence of H2ApT120.

Moreover, when tethered to the LacO array, EGFP-LacI-Bub1-K but not EGFP-LacI-Bub1-K-D946N generated H2ApT120 and recruited Sgo1 in interphase cells (Fig. 1, F and G). Importantly, EGFP-LacI-Bub1-K, but not EGFP-LacI-Bub1-K-D946N, recruited Aurora B to the LacO array on the chromosome in cells that were arrested in mitosis by the microtubule destabilizer nocodazole (Fig. 1 H). Similar results were observed when EGFP-LacI-Bub1-K–expressing cells were treated with 5-iodotubercidin (5-ITu; Fig. 1 I), a potent and selective small-molecule inhibitor of Haspin (De Antoni et al., 2012; Wang et al., 2012). Furthermore, expression of EGFP-LacI-Bub1-K could not recruit Aurora B to the LacO array when endogenous Sgo1 was depleted by siRNA (Fig. 1 J). Thus, H2ApT120 is sufficient to recruit Aurora B in mitotic cells lacking H3pT3, likely through the binding of Sgo1 to Borealin.

Taken together, our observation that either H3pT3 or H2ApT120 is sufficient to recruit Aurora B suggests that the CPC may not need to bind H3pT3 and H2ApT120 simultaneously to localize to centromeres.

Disrupting the H3pT3–Survivin interaction increases H2ApT120 and Sgo1 at metaphase centromeres

Structural analysis revealed that the BIR domain of Survivin binds H3pT3 through side chains of Lys-62 and His-80 that are hydrogen bonded with the phosphate, and that the ring nitrogen of His-80 forms a hydrogen bond with the carbonyl group of Ala-1 of H3 (Du et al., 2012; Jeyaprakash et al., 2011; Niedzialkowska et al., 2012). Therefore, these two residues (K62 and H80) are crucial for the phospho-specific binding of Survivin to H3. When endogenous Survivin was stably depleted by CRISPR/Cas9-mediated genome editing, the stably expressed Survivin mutants with Myc-tag (Survivin-K62A-Myc and Survivin-H80A-Myc) are largely impaired in supporting Aurora B localization at centromeres (Liang et al., 2018).

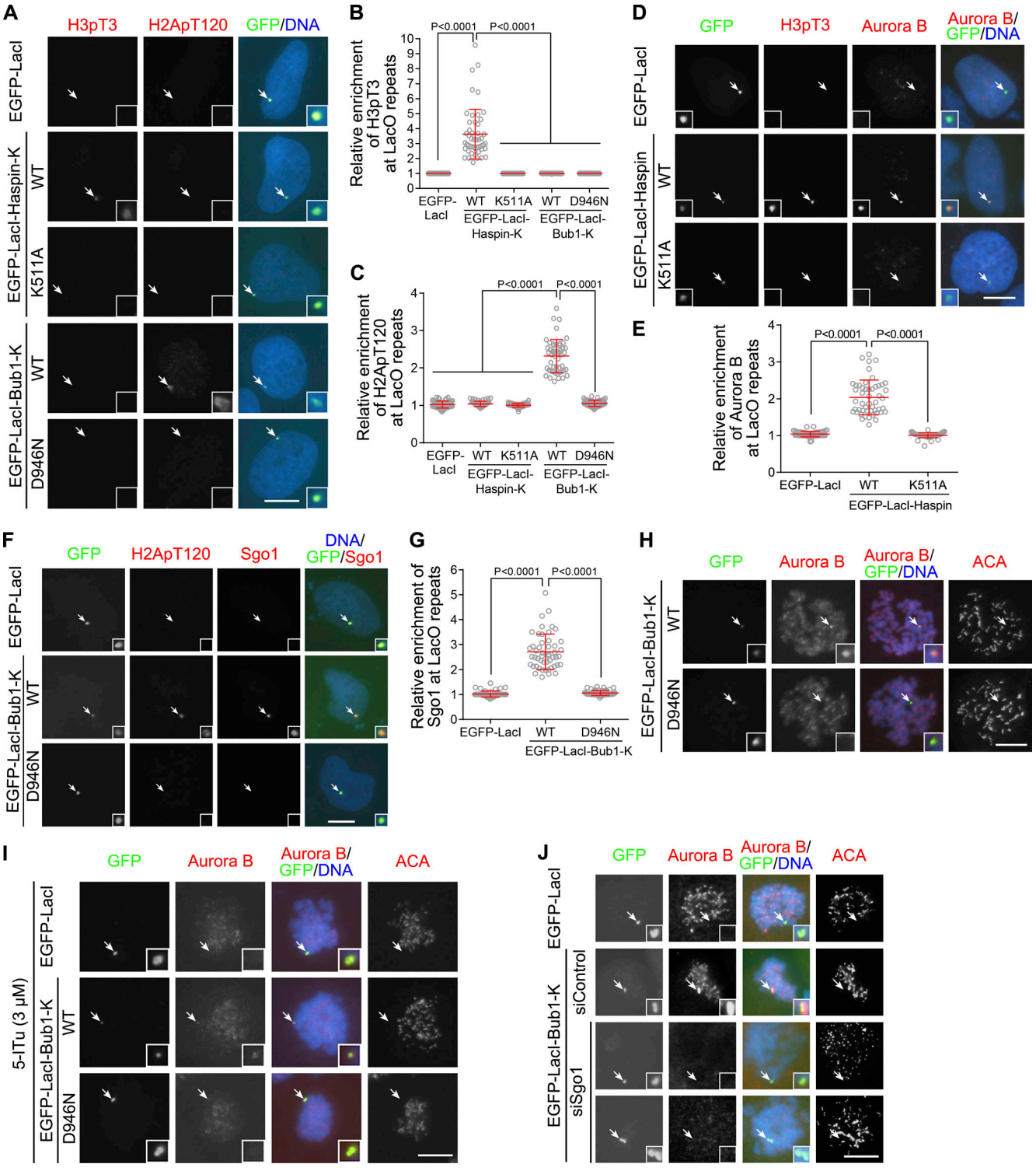

Figure 1. **Either H3pT3 or H2ApT120 alone is sufficient to recruit Aurora B. (A–C)** U2OS-LacO cells expressing EGFP-LacI, EGFP-LacI-Haspin-K, or EGFP-LacI-Bub1-K (WT or kinase-dead) were fixed and then subjected to immunofluorescence staining with DAPI and antibodies for H3pT3 and H2ApT120. Example images are shown (A). The relative enrichment of H3pT3 (B) and H2ApT120 (C) at the LacO repeats was quantified in 50 cells. **(D and E)** U2OS-LacO cells expressing WT or the kinase-dead mutant of EGFP-LacI-Haspin were fixed for immunostaining. Example images are shown (D). The relative enrichment of Aurora B at the LacO repeats was quantified in 50 cells (E). **(F and G)** U2OS-LacO cells expressing EGFP-LacI or EGFP-LacI-Bub1-K (WT or kinase-dead) were fixed for immunostaining. Example images are shown (F). The relative enrichment of Sgo1 at the LacO repeats was quantified in 50 cells (G). **(H)** U2OS-LacO cells expressing EGFP-LacI-Bub1-K (WT or kinase-dead) were exposed to nocodazole for 3 h. Mitotic cells were cytospun onto coverslips, fixed, and subjected to immunofluorescence staining with DAPI, ACA, and the antibody for Aurora B. Example images are shown. **(I)** U2OS-LacO cells expressing the indicated EGFP-LacI fusion proteins were exposed to nocodazole and 5-ITu for 3 h. Mitotic cells were cytospun onto coverslips and fixed for immunostaining as in H. **(J)** U2OS-LacO cells expressing the indicated EGFP-LacI fusion proteins and transfected with control siRNA or Sgo1 siRNA were exposed to nocodazole for 3 h. Mitotic cells were cytospun onto coverslips and fixed for immunostaining as in H. Means and SDs are shown (B, C, E, and G; unpaired *t* test). Arrows point to the LacO array. Scale bars, 10 µm.

Fluorescence microscopy showed that H2ApT120 was highly enriched at prometaphase centromeres and was then largely reduced at metaphase centromeres in control cells exogenously expressing WT Survivin (Survivin-WT-Myc; Fig. 2, A–C), which is expected (Kawashima et al., 2010). Moreover, the level of H2ApT120 at prometaphase kinetochores was comparable in control cells and cells expressing Survivin-K62A-Myc or Survivin-H80A-Myc. Strikingly, H2ApT120 at metaphase kinetochores was clearly lower in control cells than in Survivin mutant cells, indicating that the normal decline in H2ApT120 at metaphase centromeres is impeded in the absence of H3pT3–Survivin interaction. Consistent with the role of H2ApT120 in recruiting Sgo1 to centromeres, loss of the H3pT3–Survivin interaction caused an increase in the centromeric localization of Sgo1 during metaphase but not prometaphase (Fig. 2, A, D, and E). Similar results were observed when HeLa cells were treated with 5-ITu (Fig. 2, F–J). Together, these results indicate that, through binding Survivin, H3pT3 promotes the timely dephosphorylation of H2ApT120 and release of Sgo1 at metaphase centromeres.

Disrupting the H3pT3–Survivin interaction reveals an H2ApT120-dependent pool of Aurora B at the KT-proximal centromere

Given the capability of H2ApT120 in binding Sgo1 and recruiting the CPC, we were prompted to analyze the precise localization of Aurora B on chromosome spreads prepared from cells briefly arrested in metaphase with the proteasome inhibitor MG132. As in control HeLa cells, Aurora B was highly enriched at the inner centromere in cells expressing Survivin-WT-Myc and was mainly observed as a single focus between the sister CENP-C dot pair, a component protein of the CCAN at the inner kinetochore (Fig. 3 A). Strikingly, in cells expressing Survivin-K62A-Myc or Survivin-H80A-Myc, Aurora B tended to appear as two relatively weak foci at the outer edge of centromere proximal to CENP-C. This pool of Aurora B at the KT-proximal centromere was also observed when Haspin-mediated H3pT3 was inhibited by 5-ITu in MG132-arrested metaphase HeLa cells (Fig. 3 B) and nocodazole-arrested mitotic HeLa cells (Fig. 3 C).

We further found that Aurora B frequently colocalized with H2ApT120 at the KT-proximal centromere in nocodazole-arrested mitotic HeLa cells treated with 5-ITu (Fig. 3 D), implying that H2ApT120 may be involved in localizing Aurora B to the KT-proximal centromere. Indeed, when H2ApT120 was abolished by treatment with BAY 1816032, a recently developed small-molecular inhibitor of Bub1 kinase (Siemeister et al., 2019), Aurora B was no longer enriched at centromeres in Survivin mutant cells and 5-ITu-treated HeLa cells (Fig. 3, A–D). Thus, disrupting the H3pT3–Survivin interaction reveals a pool of Aurora B that is present at the KT-proximal centromere, presumably through interacting with H2ApT120-bound Sgo1.

Disrupting the H3pT3–Survivin interaction delays metaphase–anaphase transition in a Bub1-dependent way

We next determined the impact of loss of the H3pT3–Survivin interaction on mitosis progression. To allow live imaging by fluorescence microscopy, we stably expressed histone H2B C-terminally fused to GFP (H2B-GFP) in cells expressing Survivin-WT-Myc or the K62A and H80A mutants (Fig. S1 A). Time-lapse live imaging showed that the time required for the transition from nuclear envelope breakdown (NEB) to the accomplishment of metaphase chromosome alignment was comparable in Survivin-WT-Myc cells and mutant cells (Fig. 4, A and B; Fig. S1, B and C; and Videos 1, 2, and 3). In contrast, compared with that in cells expressing Survivin-WT-Myc, the time required for the transition from the completion of metaphase chromosome alignment to anaphase onset was significantly increased in Survivin mutant cells. We observed a similar delay in the metaphase–anaphase transition, but not the NEB–metaphase transition, when HeLa cells stably expressing H2B-GFP were treated with 5-ITu (Fig. 4 C; Fig. S1, D and E; and Videos 4, 5, and 6). Moreover, when cells were released from transient metaphase arrest induced by MG132 treatment, there was a dose-dependent delay in the onset of anaphase chromosome segregation in the presence of 5-ITu (Fig. 4, D and E; and Videos 7 and 8). In addition, 5-ITu treatment delayed the metaphase–anaphase transition in cells expressing Survivin-WT-Myc but not Survivin-H80A-Myc (Fig. S1, F and G), validating the specificity of the phenotype.

We further examined the effect of BAY 1816032 on mitosis progression. Treatment of HeLa cells with BAY 1816032 increased the time required for metaphase chromosome alignment but not the metaphase–anaphase transition (Fig. S1, H–J; and Videos 9 and 10), which is in line with a role for Bub1 kinase activity in promoting the efficiency of chromosome alignment (Baron et al., 2016). Interestingly, though BAY 1816032 caused a delay in the NEB–metaphase transition, it restored the proper timing for metaphase–anaphase transition in cells expressing Survivin-H80A-Myc (Fig. 4, F and G; and Fig. S1 K). Similarly, simultaneous treatment of HeLa cells with 5-ITu and BAY 1816032 caused a delay in NEB–metaphase transition but not in the metaphase–anaphase transition (Fig. 4, H and I; and Fig. S1 L).

Therefore, loss of H3pT3–Survivin interaction delays metaphase–anaphase transition in a Bub1-dependent manner, raising the possibility that H2ApT120-dependent localization of Aurora B at the KT-proximal centromere influences silencing of the SAC.

Disrupting the H3pT3–Survivin interaction hampers the removal of SAC proteins from metaphase kinetochores

Bubs are largely released from kinetochores to allow SAC silencing (London and Biggins, 2014). We therefore investigated the kinetochore localization of Bubs in cells lacking the H3pT3–Survivin interaction. As expected, Bub1 (Fig. 5, A and B) and Bub3 (Fig. S2, A and B) localized to prometaphase kinetochores and were largely released from metaphase kinetochores in Survivin-WT-Myc cells. The levels of Bubs at prometaphase kinetochores in Survivin mutant cells were comparable to those in Survivin-WT-Myc cells, indicating that SAC activation is normal in the absence of H3pT3–Survivin interaction. Interestingly, at metaphase kinetochores, the levels of Bub1 and Bub3 were higher in Survivin mutant cells than in Survivin-WT-Myc cells. These results are in line with the increased H2ApT120 in metaphase cells lacking the H3pT3–Survivin interaction (Fig. 2, A–C and F–H). Similarly, treatment of HeLa cells with 5-ITu increased the kinetochore localization of Bub3 (Fig. 5, C and D) and BubR1 (Fig. S2, C and D) during metaphase but not

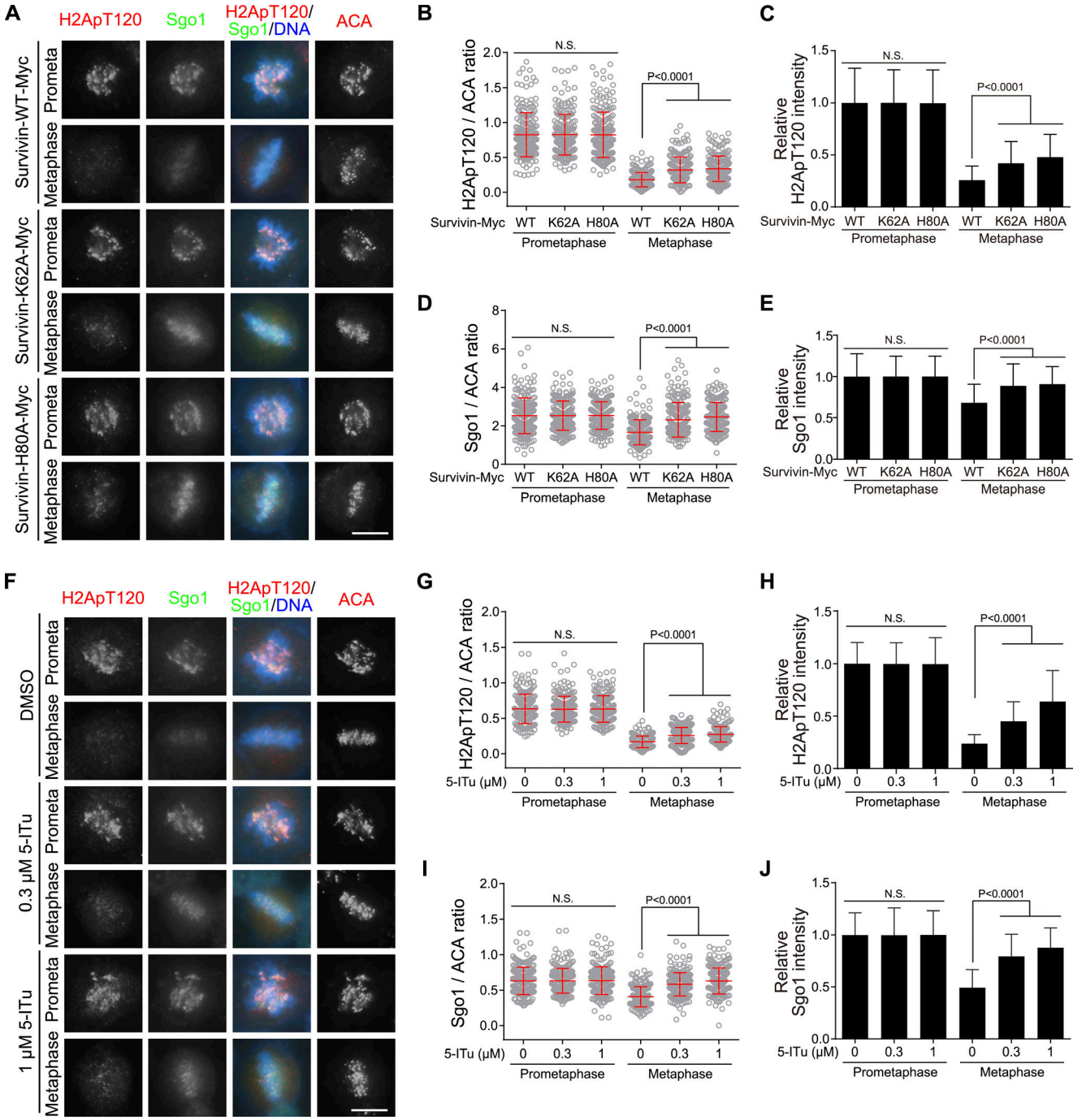

Figure 2. **Disrupting the H3pT3–Survivin interaction increases H2ApT120 and Sgo1 at metaphase centromeres. (A–E)** HeLa cells stably expressing the indicated Survivin proteins were released from STB for 12 h and then immunostained. Example images are shown (A). For each experiment, the immunofluorescence intensity ratios of H2ApT120/ACA (B) and Sgo1/ACA (D) were determined from 200 chromosomal regions containing >600 centromeres in 20 cells. The relative intensities of H2ApT120 (C) and Sgo1 (E), representing the normalized ratios of H2ApT120/ACA and Sgo1/ACA, were determined in 60 cells from three independent experiments (20 cells per experiment). **(F–J)** DMSO or 5-ITu was added to HeLa cells 9 h after release from STB. Cells were then fixed 12 h after release for immunostaining. Example images are shown (F). For each experiment, the immunofluorescence intensity ratios of H2ApT120/ACA (G) and Sgo1/ACA (I) were determined from 200 chromosomal regions containing >600 centromeres in 20 cells. The relative intensities of H2ApT120 (H) and Sgo1 (J), representing the normalized ratios of H2ApT120/ACA and Sgo1/ACA, were determined in 60 cells from three independent experiments (20 cells per experiment). Means and SDs are shown (B–E and G–J; unpaired *t* test). N.S., not significant. Scale bars, 10 μm.

prometaphase. In addition, 5-ITu was able to increase the metaphase kinetochore localization of Bubs in Survivin-WT-Myc cells but not in the Survivin mutant cells (Fig. S2, E–H). Furthermore, treatment with BAY 1816032 eliminated the localization of Bub3 and Bub1 at metaphase kinetochores in cells expressing either WT or the mutant forms of Survivin-Myc (Fig. 5, E–G) but did not affect their localization at prometaphase kinetochores (Fig. 5, H–J).

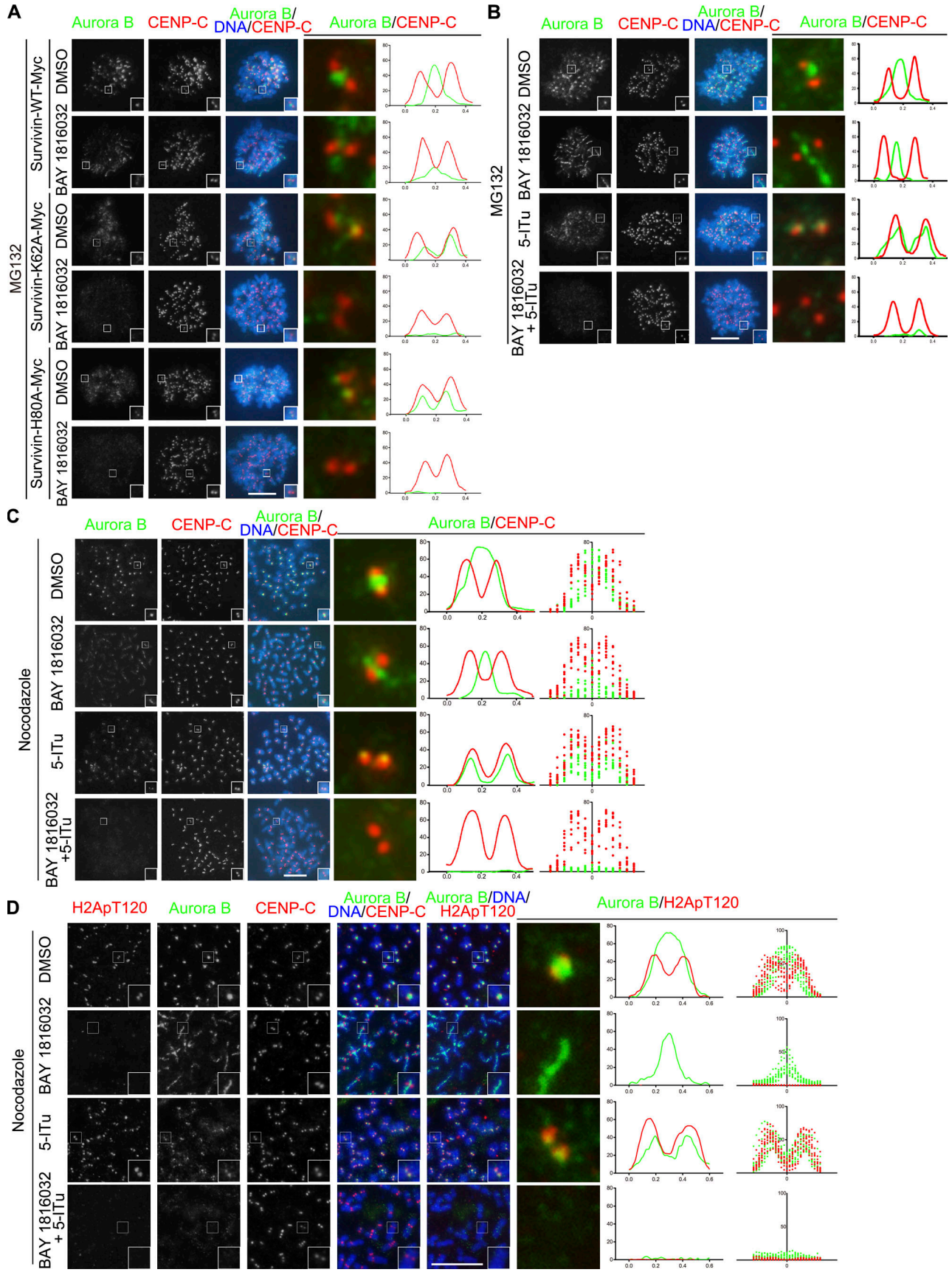

Figure 3. **Disrupting the H3pT3–Survivin interaction reveals an H2ApT120-dependent pool of Aurora B at the KT-proximal centromere. (A)** DMSO or BAY 1816032 was added to the indicated Survivin stable cell lines 9 h after release from STB, and then MG132 was added 10 h after release. Chromosome

spreads were prepared from mitotic cells collected 15 h after release and then immunostained. **(B)** DMSO or the indicated inhibitors was added to HeLa cells 7 h after release from STB, and MG132 was added 10 h after release. Chromosome spreads were prepared and immunostained as described in A. **(C)** Nocodazole and DMSO or the indicated inhibitors were added to HeLa cells 9 h after release from STB. Chromosome spreads were prepared from mitotic cells collected 12 h after release and then immunostained. Line plots and scatter plots show the fluorescence intensity across a sister kinetochore pair for Aurora B and the inner kinetochore marker CENP-C on 1 chromosome and 10 chromosomes, respectively. **(D)** Nocodazole and DMSO or the indicated inhibitors were added to HeLa cells 9 h after release from STB. Chromosome spreads were prepared and immunostained as described in C. Line plots and scatter plots show the fluorescence intensity across a sister kinetochore pair for Aurora B and H2ApT120 on 1 chromosome and 10 chromosomes, respectively. Scale bars, 10 µm.

Thus, release of Bubs from metaphase kinetochores in cells lacking the H3pT3–Survivin interaction is hampered in a Bub1 kinase activity–dependent manner, which may account for the prolonged metaphase in these cells and suggest a delay in SAC silencing.

Disrupting the H3pT3–Survivin interaction hinders dephosphorylation of Knl1-MELT motifs at metaphase kinetochores in a Bub1-dependent way

While Mps1-mediated phosphorylation of Knl1-MELT motifs recruits Bubs to kinetochores during prometaphase, dephosphorylation of Knl1-MELT at metaphase kinetochores causes the release of Bubs (Musacchio, 2015). The delay in releasing Bubs from metaphase kinetochores in cells lacking H3pT3–Survivin interaction prompted us to examine the level of Knl1-MELT phosphorylation (Knl1-pMELT) therein, using the antibody specific for phosphorylated Thr-180 in one of the MELT repeats of human Knl1 (Pachis et al., 2019).

We found that Knl1 localized normally to kinetochores in cells expressing WT or the mutant forms of Survivin-Myc (Fig. S3, A and B), as well as in cells treated with 5-ITu (Fig. S3, C and D), indicating that the H3pT3–Survivin interaction is dispensable for outer kinetochore assembly. Strikingly, compared with that in control cells, Knl1-pMELT at metaphase kinetochores was clearly elevated in cells expressing the Survivin mutants (Fig. 6, A and B) or treated with 5-ITu (Fig. 6, C and D). In addition, 5-ITu treatment increased Knl1-pMELT at metaphase kinetochores in cells expressing Survivin-WT-Myc but not Survivin-H80A-Myc (Fig. S3, E and F). Furthermore, treatment with BAY 1816032 largely eliminated Knl1-pMELT at metaphase kinetochores in cells expressing Survivin-WT-Myc or the mutants, whereas little effect was observed on Knl1-pMELT at prometaphase kinetochores (Fig. 6, E–G). Thus, retention of both Knl1-pMELT and Bubs at metaphase kinetochores in cells lacking the H3pT3–Survivin interaction requires Bub1 kinase activity.

These results indicate that dephosphorylation of Knl1-MELT during metaphase is hindered when the H3pT3–Survivin interaction is lost, which is expected to interfere with the release of Bubs from metaphase kinetochores and might contribute to a defect in SAC silencing.

Disrupting the H3pT3–Survivin interaction impedes the dephosphorylation of Knl1-RVSF motif at metaphase kinetochores in a Bub1-dependent manner

Dephosphorylation of Knl1-MELT in metaphase depends on PP1γ (Nijenhuis et al., 2014), which is recruited to metaphase kinetochores through binding Knl1, whereas the Knl1–PP1γ interaction is inhibited by Aurora B–mediated phosphorylation of Knl1 at the RVSF motif (Knl1-pRVSF). We examined whether loss of H3pT3–Survivin interaction affects Knl1-pRVSF, using the antibody specific for phosphorylated Ser-60 in the RVSF motif of human Knl1 (Welburn et al., 2010).

We found comparable levels of Knl1-pRVSF at prometaphase kinetochores in cells expressing Survivin-WT-Myc and the mutants (Fig. 7, A and B). Moreover, compared with that at prometaphase kinetochores, Knl1-pRVSF at metaphase kinetochores was strongly reduced in cells expressing Survivin-WT-Myc, which is expected (Welburn et al., 2010). Strikingly, Knl1-pRVSF at metaphase kinetochores was largely retained in cells expressing the Survivin mutants. Similarly, treatment of HeLa cells with 5-ITu did not affect Knl1-pRVSF at prometaphase kinetochores, but significantly increased Knl1-pRVSF at metaphase kinetochores (Fig. 7, C and D). 5-ITu increased Knl1-pRVSF at metaphase kinetochores in cells expressing Survivin-WT-Myc but not Survivin-H80A-Myc (Fig. S4, A and B), validating the specificity of the effect. Furthermore, BAY 1816032 did not affect Knl1-pRVSF at prometaphase kinetochores in cells expressing Survivin-WT-Myc or the mutants (Fig. 7, E and F). In contrast, BAY 1816032 treatment prevented the increase in Knl1-pRVSF at metaphase kinetochores in Survivin mutant cells (Fig. 7, E and G). We observed similar results for the phosphorylation of Knl1-SSILK motif (Knl1-pSSILK; Fig. S4, C–E), using the antibody for phosphorylated Ser-24 in the SSILK motif of human Knl1 (Welburn et al., 2010), indicating that the phenotype is not specific for Knl1-pRVSF.

Thus, loss of H3pT3–Survivin interaction impedes the dephosphorylation of Knl1-RVSF at metaphase kinetochores in a way dependent on Bub1 kinase activity, which is likely the cause for the delay in dephosphorylating Knl1-MELT during metaphase.

Disrupting the H3pT3–Survivin interaction does not delay metaphase Knl1 dephosphorylation and SAC silencing in cells lacking H2ApT120-bound Sgo1

The above results suggest that H2ApT120-dependent accumulation of Aurora B at the KT-proximal centromere might be responsible for retaining Knl1-pRVSF at metaphase kinetochores in cells lacking the H3pT3–Survivin interaction. In line with the role for H2ApT120-bound Sgo1 in recruiting the CPC (Tsukahara et al., 2010), Sgo1 tethered to the LacO array as a fusion protein with Myc-tagged LacI (Sgo1-Myc-LacI) recruited INCENP to the LacO array on the mitotic chromosome in U2OS-LacO cells (Fig. S5 A). Similar results were observed in 5-ITu–treated mitotic U2OS-LacO cells expressing EGFP-LacI–fused Sgo1 (EGFP-LacI-Sgo1; Fig. S5 B).

We thus wondered whether disrupting the H3pT3–Survivin interaction could impede the dephosphorylation of Knl1-RVSF at metaphase kinetochores in cells where Sgo1 is incapable of binding H2ApT120. To test this possibility, we used a previously established HeLa-derived cell line in which the Lys-492 to Ala

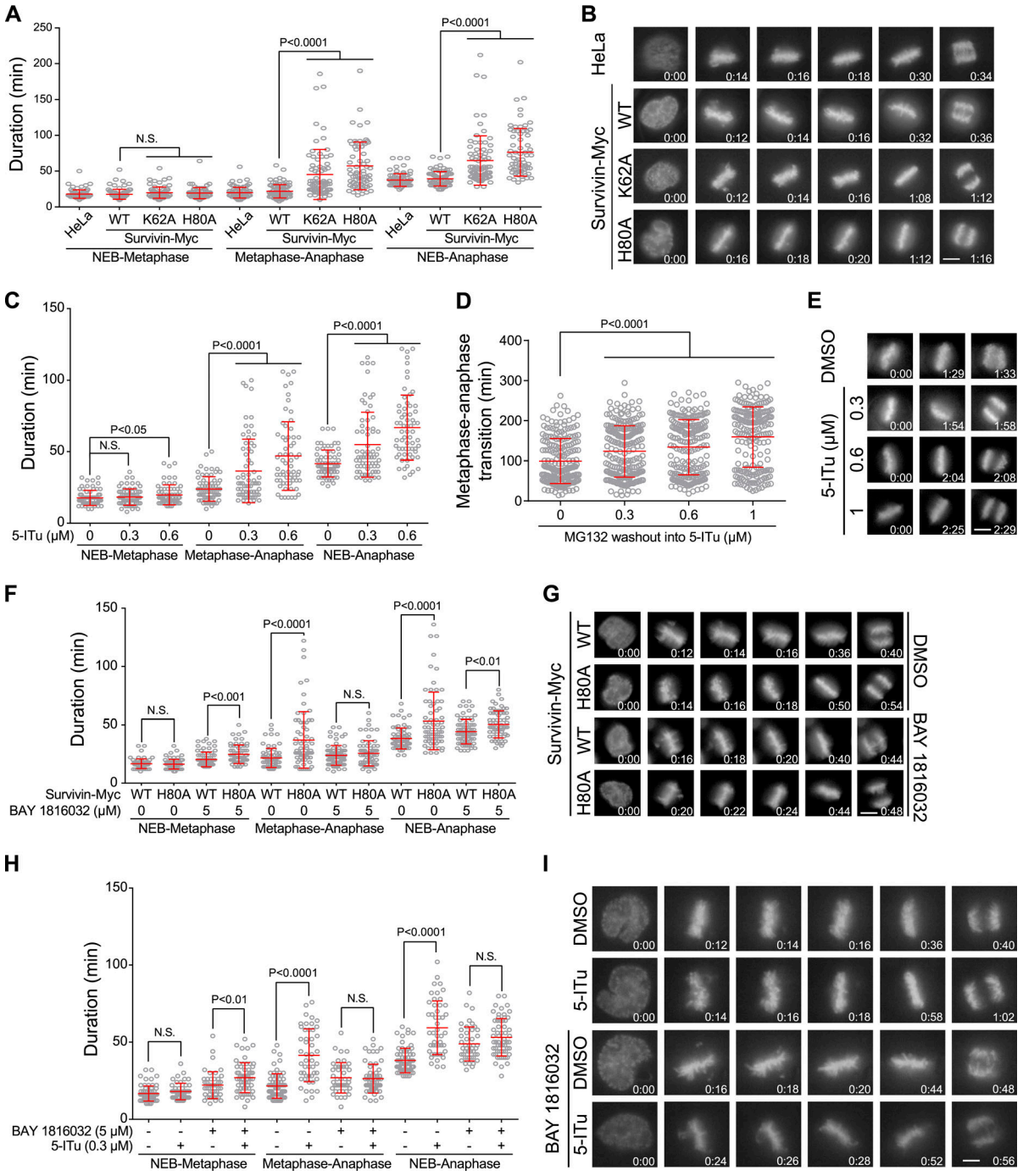

Figure 4. **Disrupting the H3pT3–Survivin interaction delays metaphase–anaphase transition in a Bub1-dependent way. (A and B)** HeLa and the indicated Survivin cell lines stably expressing H2B-GFP were released from STB, and then mitosis progression was analyzed by time-lapse live imaging. The time from NEB to metaphase chromosome alignment and from metaphase to anaphase onset was determined in ≥66 cells (A). Selected frames of the videos are shown (B). See also Videos 1, 2, and 3. **(C)** DMSO or 0.3–0.6 µM 5-ITu was added to HeLa cells stably expressing H2B-GFP 7 h after release from STB, and then mitosis progression was analyzed in ≥64 cells. See also Videos 4, 5, and 6. **(D and E)** MG132 was added to HeLa cells stably expressing H2B-GFP 10.5 h after release from STB. After 2-h incubation in MG132, cells were released into DMSO or 0.3–1.0 µM 5-ITu, and then mitosis progression was analyzed by time-lapse live imaging. The time from MG132 release to anaphase onset was determined in ≥200 cells (D). Selected frames of the videos are shown (E). See also Videos 7 and 8. **(F and G)** DMSO or BAY 1816032 was added to the indicated Survivin cell lines stably expressing H2B-GFP 7 h after release from STB, and then mitosis progression was analyzed in ≥66 cells (F). Selected frames of the videos are shown (G). **(H and I)** DMSO or the indicated inhibitors was added to HeLa cells stably expressing H2B-GFP at 7 h after release from STB, and then mitosis progression was analyzed in ≥45 cells (H). Selected frames of the videos are shown (I). Means and SDs are shown (A, C, D, F, and H; unpaired *t* test). N.S., not significant. Time stated in h:min. Scale bars, 10 µm. See also Fig. S1.

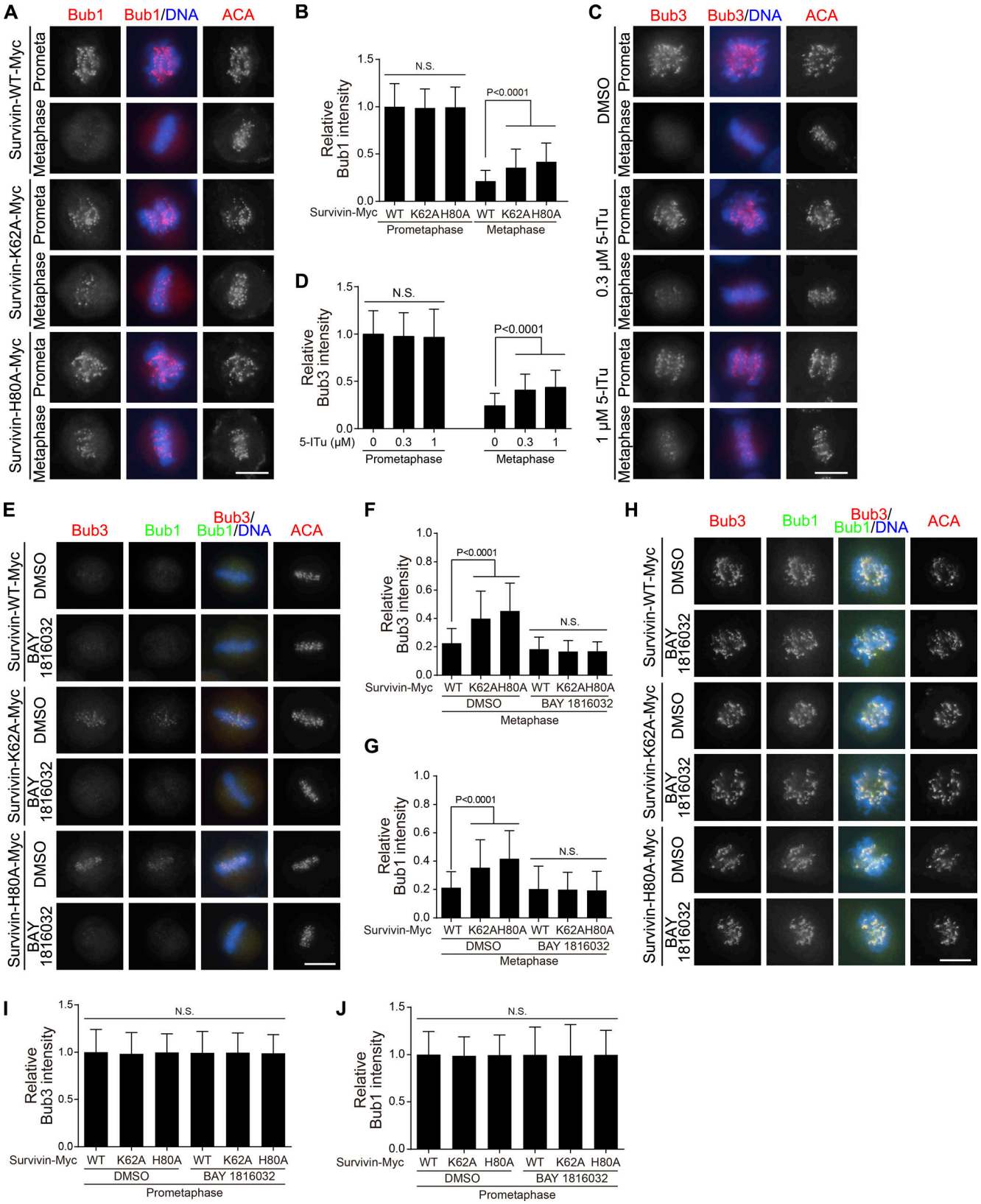

Figure 5. **Disrupting the H3pT3–Survivin interaction hampers the removal of SAC proteins from metaphase kinetochores. (A and B)** The indicated Survivin stable cell lines were released from STB for 12 h and then immunostained. Example images are shown (A). The relative intensity of Bub1, representing the normalized ratio of Bub1/ACA, was determined in 60 cells from three independent experiments (20 cells per experiment; B). **(C and D)** DMSO or 5-ITu was added to HeLa cells 7 h after release from STB. Cells were then fixed 12 h after release for immunostaining. Example images are shown (C). The relative intensity of Bub3 was determined as in B (D). **(E–G)** DMSO or BAY 1816032 was added to the indicated Survivin stable cell lines 9 h after release from STB. Cells

were then fixed 12 h after release for immunostaining. Example images are shown (E). The relative intensity ratios of Bub3 (F) and Bub1 (G) were determined as in B. **(H–J)** DMSO or BAY 1816032 was added to the indicated Survivin stable cell lines 9 h after release from STB. Cells were then fixed 12 h after release for immunostaining. Example images are shown (H). The relative intensity ratios of Bub3 (I) and Bub1 (J) were determined as in B. Means and SDs are shown (B, D, F, G, I, and J; unpaired *t* test). N.S., not significant. Scale bars, 10 µm. See also Fig. S2.

(K492A) mutation in the C-terminal basic region of Sgo1, which renders Sgo1 deficient in binding H2ApT120 and localizing to centromeres (Liu et al., 2013; Tang et al., 2006), was introduced into endogenous Sgo1 by CRISPR/Cas9-mediated genome editing (Liang et al., 2019). We previously showed that, in this cell line, Aurora B is less concentrated at the centromeres and displays diffuse signals along the length of chromosomes compared with control HeLa cells (Liang et al., 2019). Importantly, 5-ITu treatment significantly increased Knl1-pRVSF (Fig. 8, A and B) and Knl1-pMELT (Fig. 8, C and D) at metaphase kinetochores in control HeLa cells but not in Sgo1-K492A cells. Similar results were obtained for the localization of Bub1 and Bub3 at metaphase kinetochores (Fig. S5, C–G). Consistently, time-lapse live imaging demonstrated that 5-ITu delayed the metaphase–anaphase transition in control HeLa cells, but not in Sgo1-K492A cells (Fig. 8, E–G). These results indicate that H2ApT120-bound Sgo1 is responsible for delayed Knl1 dephosphorylation and SAC silencing in cells lacking the H3pT3–Survivin interaction.

Disrupting H3pT3–Survivin and H2ApT120–Sgo1 interactions additively reduces Aurora B–mediated phosphorylation of Hec1 at prometaphase kinetochores

Aurora B phosphorylates the N-terminal segment of Hec1 in early mitosis, which is important for the correction of erroneous KT-MT attachments. We next examined whether loss of centromeric Aurora B affects Hec1 phosphorylation, using the antibody specific for Hec1 Ser-44 phosphorylation (Hec1-pS44; DeLuca et al., 2011, 2018). In line with the observation that 5-ITu treatment did not affect the kinetochore localization of Hec1 in human cells (De Antoni et al., 2012), Hec1 localized normally to kinetochores in Survivin mutant cells (Fig. 9, A and B). Compared with control cells, Hec1-pS44 at prometaphase kinetochores was reduced by 14.6–18.1% in Survivin mutant cells (Fig. 9, A and C) and 5-ITu–treated HeLa cells (Fig. 9, D and E). Moreover, Hec1-pS44 was nearly undetectable at metaphase kinetochores in Survivin mutant cells (Fig. 9 A) and 5-ITu–treated HeLa cells (Fig. 9 D), as in control cells. Consistently, the cold-stable tubulin of metaphase spindle was not detectably altered in Survivin mutant cells (Fig. 9 F) and 5-ITu–treated cells (Fig. 9 G), indicative of proper stabilization of KT-MT attachment.

We further found that, compared to DMSO treatment, BAY 1816032 treatment reduced Hec1-pS44 at prometaphase kinetochores by 13.3% and 18.5% in cells expressing Survivin-WT-Myc and Survivin-H80A-Myc, respectively (Fig. 9, H and I), implying the contribution of the H2ApT120-dependent pool of Aurora B to Hec1-pS44 at prometaphase kinetochores. Moreover, compared with that in Survivin-WT-Myc cells treated with DMSO, the level of Hec1-pS44 in Survivin-H80A-Myc cells treated with BAY 1816032 was reduced by 36.7%. Taken together, these results indicate that H3pT3- and H2ApT120-dependent localization of Aurora B additively and substantially contributes to Hec1-pS44, but not Knl1-pRVSF, at prometaphase kinetochores.

Disrupting H3pT3–Survivin interaction increases chromosome missegregation in the absence of H2ApT120–Sgo1 interaction

To assess the relative functional contribution of H3pT3- and H2ApT120-dependent pathways of Aurora B recruitment, we examined chromosome segregation in cells lacking one or both pathways. Cells expressing WT or the mutant forms of Survivin-Myc had similarly low levels of anaphases with lagging chromosomes (Fig. 10, A and B). Interestingly, upon treatment with BAY 1816032, the frequency of anaphase lagging chromosomes was significantly higher in cells expressing the Survivin mutants than in Survivin-WT-Myc cells. Consistently, while treatment with 5-ITu alone barely affected chromosome segregation in HeLa cells, it strongly increased the frequency of anaphase lagging chromosomes in the presence of BAY 1816032 (Fig. 10, C and D). Similar results were obtained in the non-transformed retinal pigment epithelial-1 cells treated with 5-ITu and BAY 1816032 (Fig. 10, E and F). Therefore, the H3pT3–Survivin interaction becomes essential for the fidelity of chromosome segregation in the absence of Bub1 kinase activity.

We further assessed the effect of 5-ITu on chromosome segregation in Sgo1-K492A cells, which lack H2ApT120-dependent localization of Sgo1 and CPC at centromeres (Liang et al., 2018). Consistent with the effect of BAY 1816032 on chromosome segregation in HeLa cells (Fig. 10, A–D), the rate of anaphase lagging chromosomes was slightly higher in Sgo1-K492A cells than in control HeLa cells (Fig. 10, G and H). Importantly, 5-ITu treatment obviously increased the frequency of anaphase lagging chromosomes in Sgo1-K492A cells but not in control HeLa cells, indicating that the H2ApT120–Sgo1 interaction is required to suppress chromosome missegregation in cells lacking H3pT3.

Anaphase lagging chromosomes usually result from merotelic kinetochore attachment in which a single kinetochore is simultaneously attached to microtubules from both spindle poles. Indeed, we found that 32.3% of Survivin-H80A-Myc cells treated with BAY 1816032 had at least one merotelically attached kinetochore, which was an approximately threefold increase over control Survivin-WT-Myc cells with mock treatment (Fig. 10 I). Taken together, these results indicate that H2ApT120-dependent localization of Aurora B is required to prevent merotelic attachment and chromosome missegregation in the absence of the H3pT3-dependent pool of Aurora B.

Discussion

In this study, we investigated the role of centromere-localized Aurora B in mitotic human cells. By mutating key residues in the

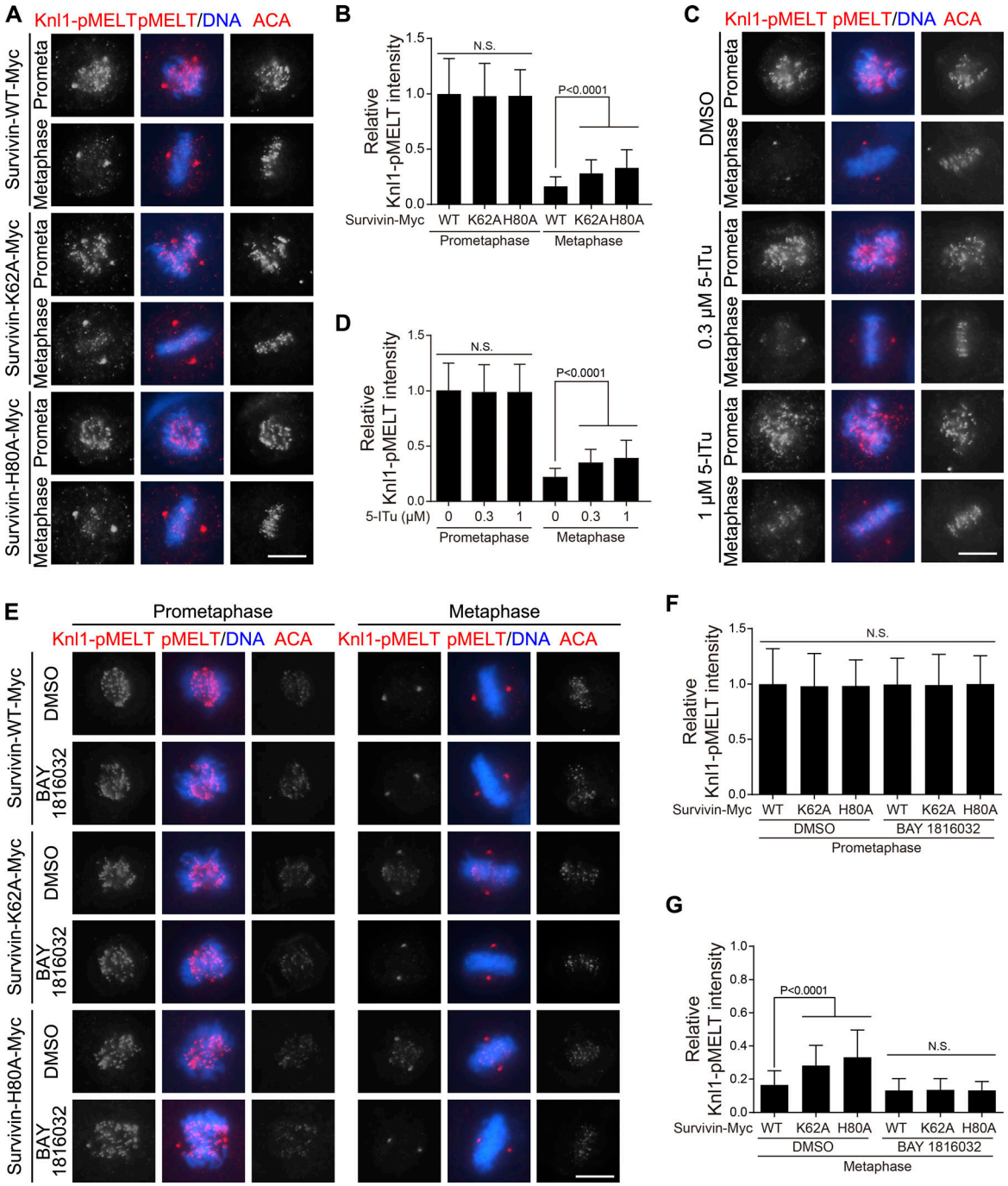

Figure 6. **Disrupting the H3pT3–Survivin interaction hinders dephosphorylation of Knl1-MELT motifs at metaphase kinetochores in a Bub1-dependent way. (A and B)** The indicated Survivin stable cell lines were released from STB for 12 h, and then immunostained. Example images are shown (A). The relative intensity of Knl1-pMELT, representing the normalized ratio of Knl1-pMELT/ACA, was determined in 60 cells from three independent experiments (20 cells per experiment; B). **(C and D)** DMSO or 5-ITu was added to HeLa cells 9 h after release from STB. Cells were then fixed 12 h after release for immunostaining. Example images are shown (C). The relative intensity of Knl1-pMELT/ACA was determined as in B (D). **(E–G)** DMSO or BAY 1816032 was added to the indicated Survivin stable cell lines 9 h after release from STB. Cells were then fixed 12 h after release for immunostaining. Example images are shown (E). The relative intensity of Knl1-pMELT/ACA in prometaphase (F) and metaphase (G) cells were determined as in B. Means and SDs are shown (B, D, F, and G; unpaired *t* test). N.S., not significant. Scale bars, 10 µm. See also Fig. S3.

H3pT3-binding BIR domain of Survivin, which disrupts the H3pT3-dependent localization of Aurora B at inner centromeres but retains proper centromeric cohesion (Liang et al., 2018), we found a pool of Aurora B at the KT-proximal centromere in prometaphase and metaphase cells. We confirmed this finding by using the Haspin kinase inhibitor 5-ITu, similar to previous observations for Borealin in 5-ITu–treated cells (Bekier et al., 2015). This pool of Aurora B persists in the presence of the

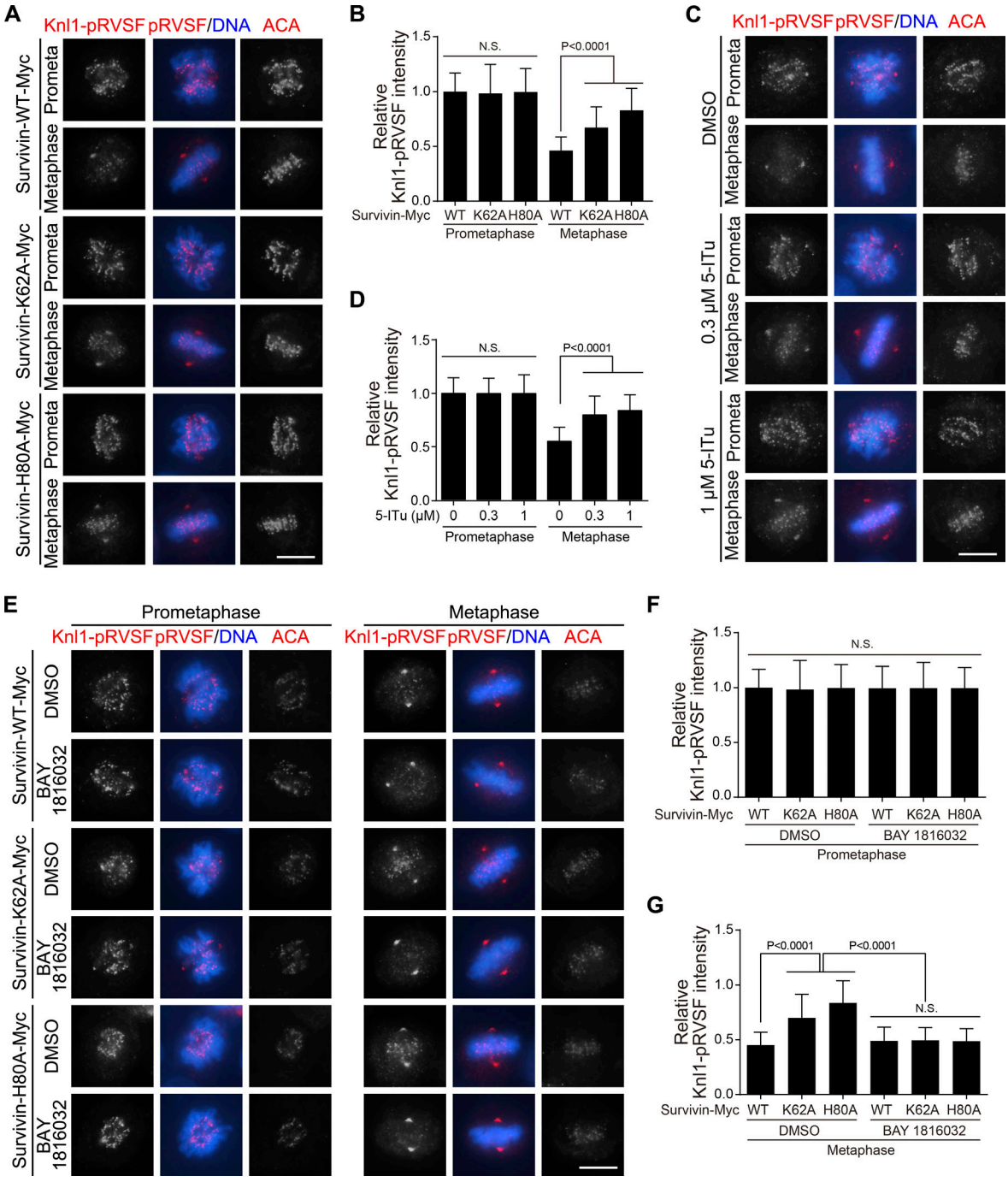

Figure 7. **Disrupting the H3pT3–Survivin interaction impedes the dephosphorylation of Knl1-RVSF motif at metaphase kinetochores in a Bub1-dependent manner. (A and B)** The indicated Survivin stable cell lines were released from STB for 12 h and then immunostained. Example images are shown (A). The relative intensity of Knl1-pRVSF, representing the normalized ratio of Knl1-pRVSF/ACA, was determined in 60 cells from three independent experiments (20 cells per experiment; B). **(C and D)** DMSO or 5-ITu was added to HeLa cells 9 h after release from STB. Cells were then fixed 12 h after release for immunostaining. Example images are shown (C). The relative intensity of Knl1-pRVSF/ACA was determined as in B (D). **(E–G)** DMSO or BAY 1816032 was added to the indicated Survivin stable cell lines 9 h after release from STB. Cells were then fixed 12 h after release for immunostaining. Example images are shown (E). The relative intensity ratio of Knl1-pRVSF/ACA in prometaphase (F) and metaphase (G) cells was determined as in B. Means and SDs are shown (B, D, F, and G; unpaired *t* test). N.S., not significant. Scale bars, 10 μm. See also Fig. S4.

spindle poison nocodazole, ruling out the involvement of CPC binding to microtubules (Banerjee et al., 2014; Fink et al., 2017; Samejima et al., 2015; van der Horst et al., 2015; Wheelock et al., 2017). We presented several lines of evidence indicating that H2ApT120-bound Sgo1 provides the docking site for Aurora B at the KT-proximal centromere. First, H2ApT120 and Sgo1 are able to recruit Aurora B even in the absence of H3pT3. Second, disrupting the H3pT3–Survivin interaction impedes the decline in

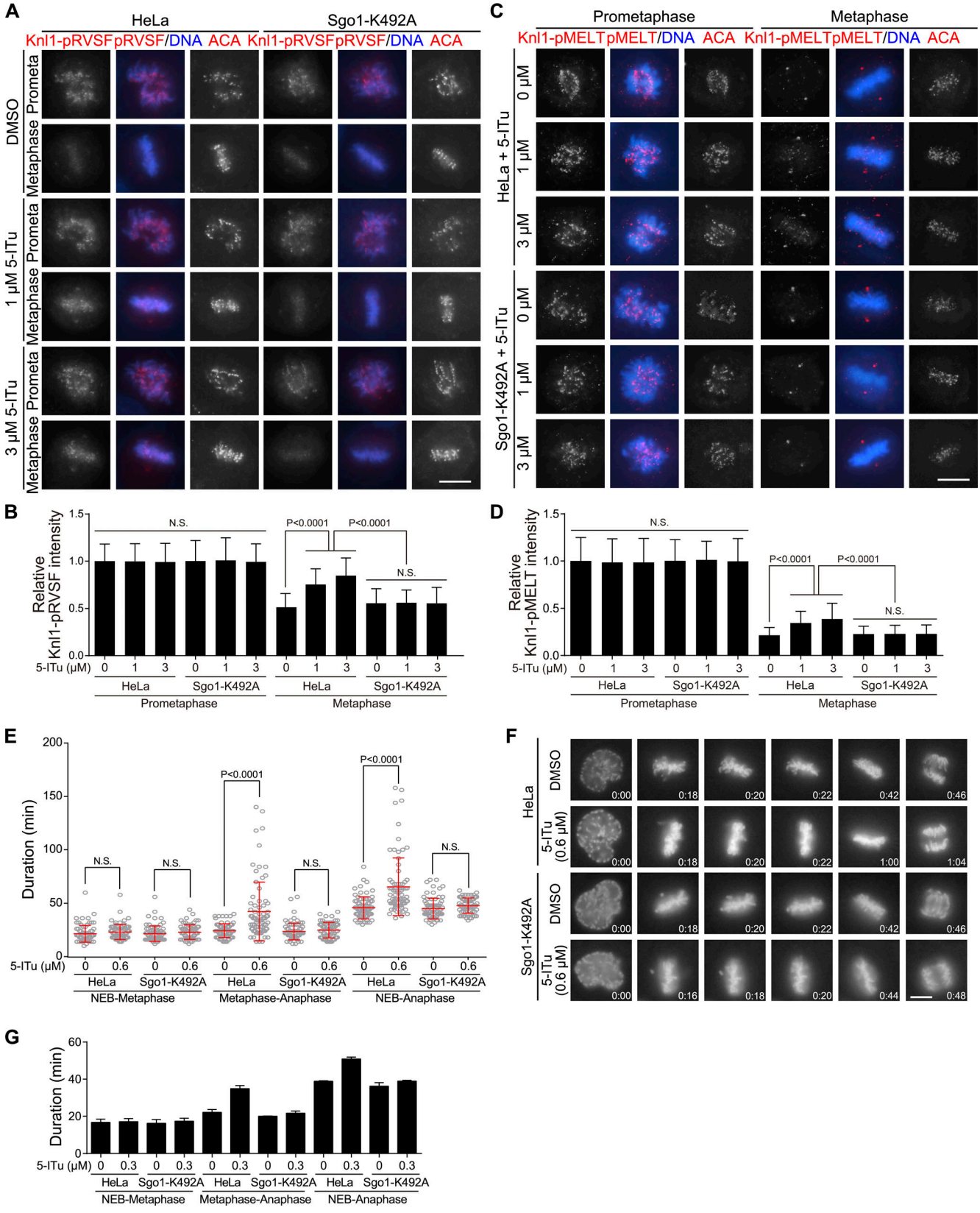

Figure 8. **Disrupting the H3pT3–Survivin interaction does not delay metaphase Knl1 dephosphorylation and SAC silencing in cells lacking H2ApT120-bound Sgo1. (A–D)** DMSO or 5-ITu was added to HeLa or the Sgo1-K492A cells 9 h after release from STB. Cells were then fixed 12 h after release for immunostaining. Example images are shown (A and C). The relative intensities of Knl1-pRVSF (B) and Knl1-pMELT (D), representing the normalized ratios of Knl1-pRVSF/ACA and Knl1-pMELT/ACA, were determined in 60 cells from three independent experiments (20 cells per experiment). **(E and F)** DMSO or 0.6 μM 5-ITu was added to HeLa or the Sgo1-K492A cells stably expressing H2B-GFP at 7 h after release from STB, and then mitosis progression was analyzed in ≥67

cells (E). Selected frames of the videos are shown (F). **(G)** DMSO or 0.3 µM 5-ITu was added to HeLa or the Sgo1-K492A cells, and then mitosis progression was analyzed as in E. The means and ranges of mitotic duration were determined in >74 cells for each condition from two independent experiments. Means and SDs are shown (B, D, E, and G; unpaired *t* test). Time stated in h:min. N.S., not significant. Scale bars, 10 µm. See also Fig. S5.

H2ApT120 and Sgo1 during metaphase, which is accompanied by accumulation of Aurora B at the KT-proximal centromere. Third, Aurora B colocalizes with H2ApT120 at the KT-proximal centromere when the H3pT3–Survivin interaction is lost. Fourth, erasing H2ApT120 by inhibiting Bub1 kinase activity, or disrupting the H2ApT120-Sgo1 interaction, removes Aurora B from the KT-proximal centromere.

Aurora B phosphorylates multiple targets within the KMN network in early mitosis, subsequent dephosphorylation of which during metaphase is important for the stabilization of KT-MT attachments and silencing of the SAC. We found that metaphase dephosphorylation of Aurora B target sites in Hec1 and Knl1 responds differentially to the loss of the centromeric CPC. We used phospho-specific antibodies that probe Aurora B activity at kinetochores at a known distance from CENP-A at the inner edge of kinetochores (Knl1-pS60 ∼80 nm and Hec1-pS44 ∼110 nm at metaphase; Wan et al., 2009; Welburn et al., 2010). We observed that, upon loss of the H3pT3-dependent pool of Aurora B at inner centromeres, Hec1-S44 is normally dephosphorylated in metaphase, whereas dephosphorylation of the Knl1-RVSF motif is significantly delayed due to the maintenance of a H2ApT120-dependent pool of Aurora B at metaphase KT-proximal centromeres. The correlation between metaphase dephosphorylation of Hec1 and Knl1 with their relative distance to the inner centromere lends support for the spatial separation model for kinetochore substrate phosphorylation by centromeric Aurora B (Lampson and Cheeseman, 2011; Liu et al., 2009; Tanaka et al., 2002; Welburn et al., 2010). However, this model cannot explain our finding that H3pT3- and H2ApT120-dependent pools of Aurora B at centromeres additively contribute to Hec1-pS44 but are not required for Knl1-pRVSF at prometaphase kinetochores. Therefore, the Knl1-RVSF motif is phosphorylated by another pool of Aurora B that may or may not reside at the kinetochore (Caldas et al., 2013; DeLuca et al., 2011).

We further found that, in cells lacking H3pT3-dependent Aurora B at inner centromeres, the enhanced phosphorylation of Knl1-RVSF/SSILK motifs at metaphase kinetochores is accompanied by defects in dephosphorylating Knl1-MELT and releasing Bubs, eventually leading to a delay in SAC silencing. Our data indicate that inhibition of PP1γ recruitment to Knl1 due to metaphase phosphorylation of the PP1-binding motif of Knl1 by H2ApT120/Sgo1-associated Aurora B is the root cause for SAC silencing delay, though we cannot fully rule out the possibility that subtle defects in KT-MT attachment may also affect SAC. Thus, regardless of whether H3pT3 and H2ApT120 may directly compete for the recruitment of the CPC to centromeres, upon loss of the H3pT3-dependent pool of Aurora B at the inner centromere, the Bub1-H2ApT120-Sgo1-CPC pathway can form a positive feedback circuit that causes the accumulation of Aurora B at metaphase kinetochores, which then feeds back to phosphorylate Knl1-RVSF and sustain Bub1 at metaphase kinetochores. These results not only represent the evidence for an indirect role of Bub1 kinase activity in inhibiting SAC silencing under certain circumstances, such as when the H3pT3-dependent pool of Aurora B at inner centromeres is lost, but also lend support for the role of PP1γ (Nijenhuis et al., 2014), as well as the B56 family of PP2A (Espert et al., 2014), in SAC silencing. Our data may also explain the metaphase delay in the cohesin releaser Wapl-depleted HeLa cells expressing centromere-targeting domain of CENP-B–fused INCENP (Hengeveld et al., 2017). We conclude that timely silencing of the SAC requires strict confinement of Aurora B to the inner centromere by H3pT3, which allows spatial separation of Knl1 from centromeric Aurora B during metaphase. We reason that cells lacking H3pT3–Survivin interaction are capable of exiting mitosis in the end because the sustained kinetochore tension eventually pulls Knl1 out of the influence of Aurora B.

Merotelic KT-MT attachment, which allows chromosome alignment on the metaphase spindle and can satisfy the SAC (Gregan et al., 2011), represents a major cause of chromosome missegregation during mitosis and is the primary mechanism of chromosomal instability in cancer cells (Thompson et al., 2010). Our data indicate that accumulation of a sufficient amount of active Aurora B at the centromere by H3pT3 and H2ApT120 makes the system robust enough to correct merotelic KT-MT attachment. Consistently, the CPC mutant incapable of localizing to centromeres is unable to correct attachment errors in *Xenopus laevis* egg extracts (Haase et al., 2017). In contrast, deletion of the N-terminal centromere-targeting domain of the INCENP homologue Sli15 (Sli15-ΔNT) did not cause severe defects in chromosome segregation in budding yeast (Campbell and Desai, 2013), which could be because merotelic attachment is not possible in this organism where there is only one microtubule-binding site on each kinetochore (Biggins, 2013). Nevertheless, metaphase chromosome alignment eventually occurs in human cells lacking both H3pT3- and H2ApT120-dependent localization of Aurora B to centromeres, though with diminished efficiency. This is in line with the observation that ∼60% residual Hec1-pS44 signal is present at prometaphase kinetochores in the absence of centromeric Aurora B. Consistently, partial inhibition of Aurora B kinase activity by a small-molecule inhibitor increased the frequency of merotelic KT-MT attachment in mammalian cells but had little effect on metaphase chromosome alignment (Cimini et al., 2006). Future studies are required to identify the pool of Aurora B that supports metaphase chromosome alignment in cells lacking the H3pT3-dependent and H2ApT120-dependent pools of Aurora B at centromeres.

In summary, we demonstrate that the H2ApT120-dependent pool of Aurora B at the KT-proximal centromere can compensate for the loss of an H3pT3-dependent pool of Aurora B at inner centromeres to correct erroneous KT-MT attachments. We suggest that this is achieved not only through maintaining a sufficient amount of residual Aurora B at the KT-proximal centromere but also by delaying the metaphase–anaphase

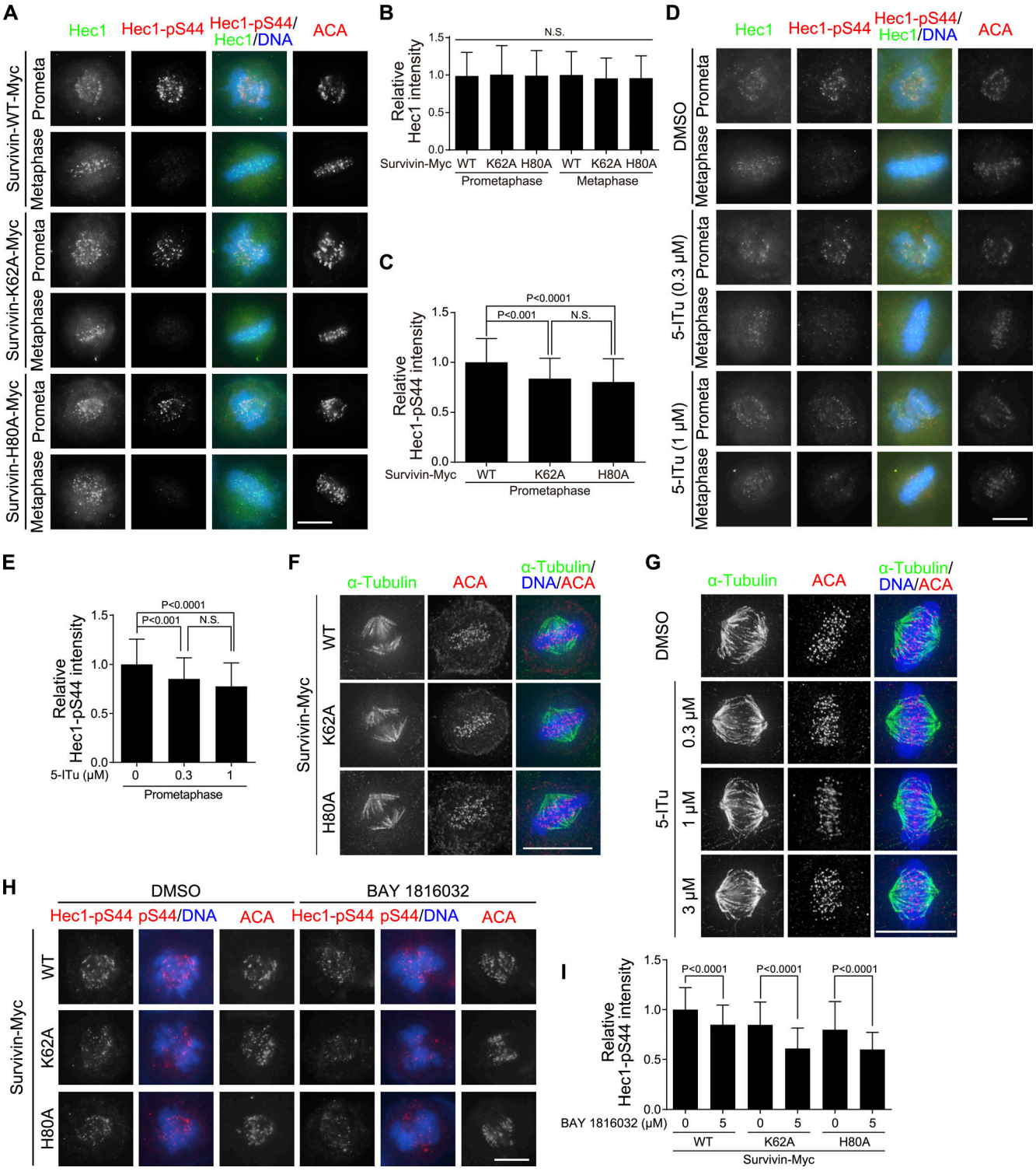

Figure 9. **Disrupting H3pT3–Survivin and H2ApT120–Sgo1 interactions additively reduces Aurora B–mediated phosphorylation of Hec1 at prometaphase kinetochores. (A–C)** The indicated Survivin stable cell lines were released from STB for 12 h and then immunostained. Example images are shown (A). The relative intensities of Hec1 (B) and Hec1-pS44 (C), representing the normalized ratios of Hec1/ACA and Hec1-pS44/ACA, were determined in 60 cells from three independent experiments (20 cells per experiment). **(D and E)** DMSO or 5-ITu was added to HeLa cells 9 h after release from STB. Cells were then fixed 12 h after release for immunostaining. Example images are shown (D). The relative intensity of Hec1-pS44 was determined as in C (E). **(F)** MG132 was added to the indicated Survivin stable cell lines 10 h after release from STB. Cells were treated with cold medium 12 h after release and then fixed and immunostained. The collected images were deconvolved and analyzed. **(G)** DMSO or 5-ITu was added to HeLa cells 9 h after release from STB, and then MG132 was added 10 h after release. Cells were treated with cold medium 12 h after release and then fixed and immunostained. The collected images were deconvolved and analyzed. **(H and I)** The indicated Survivin stable cell lines were released from STB for 12 h and then immunostained. Example images are shown (H). The relative intensity of Hec1-pS44 was determined as in C (I). Means and SDs are shown (B, C, E, and I; unpaired *t* test). N.S., not significant. Scale bars, 10 μm.

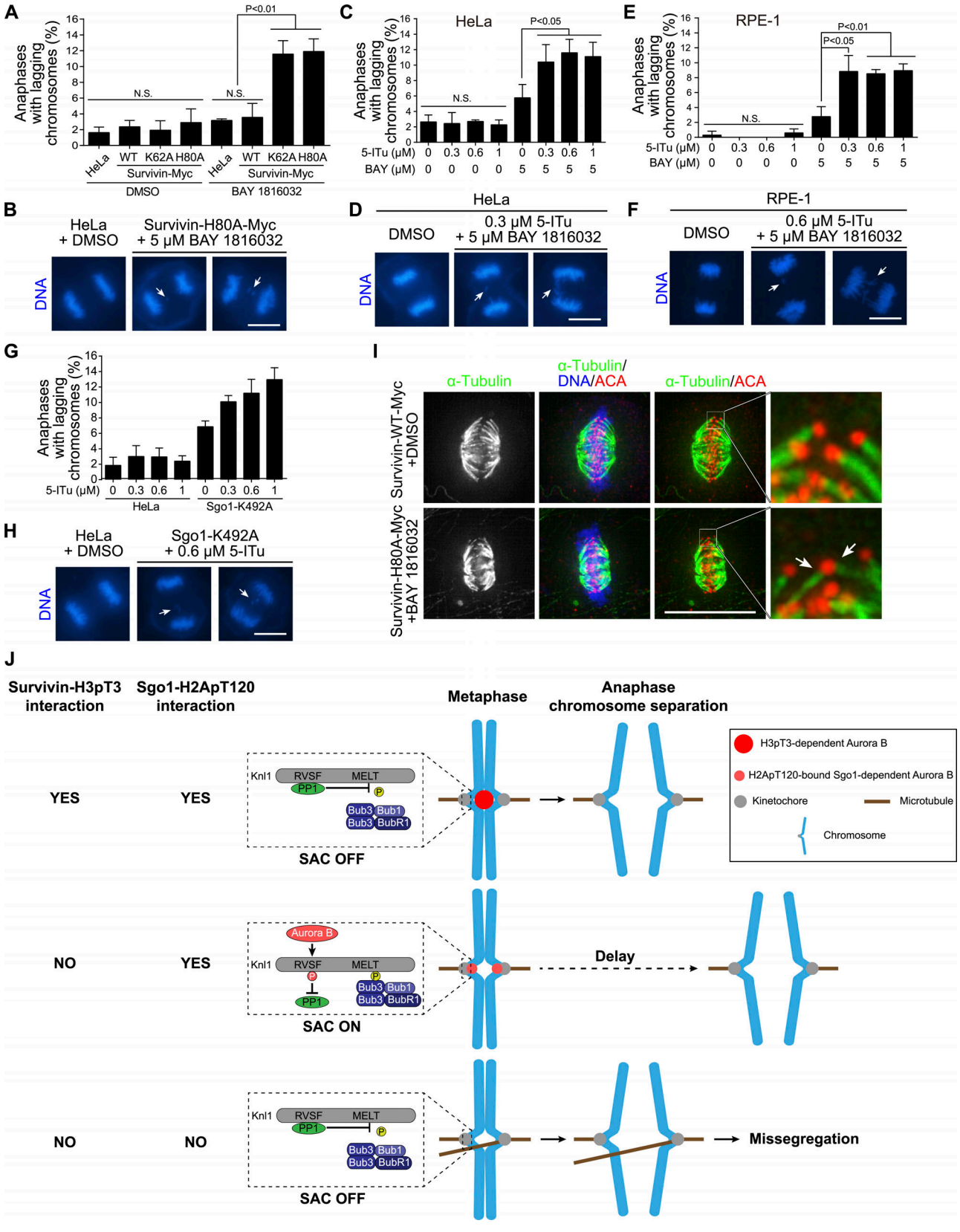

Figure 10. **Disrupting H3pT3–Survivin interaction increases chromosome missegregation in the absence of H2ApT120-Sgo1 interaction. (A and B)** DMSO or BAY 1816032 was added to HeLa cells or the indicated Survivin stable cell lines 9 h after release from STB. Cells were then fixed 12 h after release for DNA staining. The percentage of cells with lagging chromosomes was determined in >300 anaphase cells from three independent experiments (A). Example images are shown (B). **(C and D)** DMSO or the indicated inhibitors were added to HeLa cells 9 h after release from STB. Cells were then fixed 12 h after release for DNA staining. The percentage of cells with lagging chromosomes was determined in >300 anaphase cells from three independent experiments (C). Example

images are shown (D). **(E and F)** DMSO or the indicated inhibitors were added to retinal pigment epithelial-1 cells 9 h after release from STB. Cells were then fixed 12 h after release for DNA staining. The percentage of cells with lagging chromosomes was determined in >300 anaphase cells from three independent experiments (E). Example images are shown (F). **(G and H)** DMSO or 5-ITu was added to HeLa or the Sgo1-K492A cells at 9 h after release from STB. Cells were then fixed at 12 h after release for DNA staining. Means and ranges for the percentage of anaphase lagging chromosomes were determined in >200 anaphase cells from two independent experiments (G). Example images are shown (H). **(I)** DMSO or BAY 1816032 were added to the indicated Survivin stable cell lines 9 h after release from STB, and then MG132 was added 10 h after release. Cells were treated with cold medium 12 h after release and then fixed and immunostained. The collected images were deconvolved and analyzed. **(J)** Model for the role of H3pT3- and H2ApT120-dependent localization of Aurora B at centromeres in regulating kinetochore function and chromosome segregation. Means and SDs are shown (A, C, E, and G; unpaired *t* test). N.S., not significant. Arrows point to the lagging chromosome (B, D, F, and H) or the merotelic KT-MT attachment (I). Scale bars, 10 µm.

transition, thereby enabling efficient phosphorylation of outer kinetochores that drive error correction (Fig. 10 J). Similarly, two recent studies reported the existence of a pool of Aurora B/Ipl1 at the inner kinetochore that can support chromosome bi-orientation in the Sli15-ΔNT mutant yeast cells (Fischböck-Halwachs et al., 2019; Garcia-Rodriguez et al., 2019). Taken together, our results reveal the role of centromeric Aurora B in ensuring the fidelity of chromosome segregation in human cells and suggest an alternative for the model of tension sensing by spatial separation of centromeric Aurora B from kinetochore substrates (Lampson and Cheeseman, 2011; Liu et al., 2009; Tanaka et al., 2002).

Materials and methods

Cell culture, plasmids, siRNA, transfection, and drug treatments

All cells were cultured in DMEM supplemented with 1% penicillin/streptomycin and 10% FBS (Gibco) and maintained at 37°C with 5% CO_2. U2OS-LacO cells from Dr. David Spector (Cold Spring Harbor Laboratory, Cold Spring Harbor, NY) were maintained in the presence of 100 µg/ml hygromycin (Sigma-Aldrich). HeLa cells stably expressing pEF6-Survivin-Myc-6xHis in which endogenous Survivin was knocked out by CRISPR/Cas9 were maintained in 2 µg/ml blasticidin (Sigma-Aldrich). These Survivin stable cell lines were further cotransfected with pBos-H2B-GFP (Clontech) and pTRE2 (Clontech) in a 9:1 ratio, and then the clonal cell lines were selected with 1 µg/ml puromycin (Thermo Fisher Scientific). Regular HeLa cells and HeLa-derived Sgo1-K492A cells stably expressing H2B-GFP were maintained in 2 µg/ml blasticidin.

To make the EGFP-LacI fusion constructs, the PCR fragments of Bub1, Haspin, or Sgo1 were inserted into the BsiWI/BamHI sites of pSV2-EGFP-LacI. EGFP-LacI-Bub1-K (WT or D946N) contained residues 630–1,085 of Bub1 including the kinase domain. EGFP-LacI-Haspin (WT or K511A) contained full-length Haspin. EGFP-LacI-Haspin-K (WT or K511A) contained the kinase domain of Haspin (residues 471–798). EGFP-LacI-Sgo1 contained full-length Sgo1. Sgo1-Myc-LacI was constructed based on the Myc-LacI-Bub1 plasmid, which was kindly provided by Dr. Sabine Elowe (Université Laval, Québec, Canada; Asghar et al., 2015). All point mutations were introduced with the QuikChange II XL site-directed mutagenesis kit (Agilent Technologies). All plasmids were sequenced to verify desired mutations and absence of unintended mutations.

The control siRNA (Wang et al., 2010) and Sgo1 siRNA (5′-CAGUAGAACCUGCUCAGAAdTdT-3′; Zhou et al., 2017) were ordered from RiboBio. Plasmid and siRNA transfections were done with Fugene 6 (Promega) and Lipofectamine RNAiMAX (Invitrogen), respectively. Cells were arrested in S phase or at the G1/S boundary by single or double thymidine (2 mM, Calbiochem) treatment, respectively. Cells were arrested in prometaphase-like mitosis with 0.33 or 3.3 µM nocodazole (Selleckchem) or were arrested in metaphase with MG132 (10 µM, Sigma-Aldrich). The small-molecule inhibitors were 5-ITu (0.3–3 µM, Tocris) and BAY 1816032 (3–5 µM, Chemietech). Mitotic cells were collected by selective detachment with shake-off.

Antibodies and immunoblotting

Rabbit polyclonal antibodies used were to Cyclin B1 (clone D5C10, Sigma-Aldrich), GAPDH (14C10, Cell Signaling Technology), GFP (A11122, Invitrogen), H2ApT120 (Active Motif), Survivin (NB500-201, Novus Biologicals), INCENP (P240, Sigma-Aldrich), H3pT3 from Dr. Jonathan Higgins (Newcastle University, Newcastle upon Tyne, UK), Hec1-pS44 from Dr. Jennifer DeLuca (Colorado State University, Fort Collins, CO), Knl1-pS24 and Knl1-pS60 from Dr. Iain Cheeseman (Whitehead Institute for Biomedical Research, Cambridge, MA), and Knl1-pT180 from Dr. Geert Kops (Oncode Institute, Hubrecht Institute-KNAW, Utrecht, Netherlands). Rabbit anti-Bub1 and anti-Knl1 polyclonal antibodies were produced by immunization with the synthetic peptides NYGLPQPKNKPTGAR and MDGVSSEANEENDNIERPVRRR, respectively. Mouse monoclonal antibodies used were to Aurora B (AIM-1; BD Biosciences), Bub3 (Clone 31, BD Transduction Laboratories), BubR1 from Dr. Jakob Nilsson (University of Copenhagen, Copenhagen, Denmark), H3pT3 (16B2) from Dr. Hiroshi Kimura (Tokyo Institute of Technology, Yokohama, Japan), Hec1 (GTX70268, GeneTex), α-Tubulin (T-6047, Sigma-Aldrich), and Sgo1 (3C11, Abnova). Guinea pig polyclonal antibodies against CENP-C were from MBL (PD030). The anti-human centromere autoantibody (ACA) was from Immunovision. Secondary antibodies for immunoblotting were goat anti-rabbit or horse anti-mouse IgG-HRP (Sigma-Aldrich). Secondary antibodies for immunostaining were donkey anti-rabbit IgG-Alexa Fluor 488 or Cy3 (Jackson ImmunoResearch); anti-mouse IgG-Alexa Fluor 488 or 546 (Invitrogen) or CY5 (Jackson ImmunoResearch); anti-human IgG-Alexa Fluor 647 (Jackson ImmunoResearch); and goat anti-guinea pig IgG-Alexa Fluor 647 (Invitrogen). SDS-PAGE and immunoblotting were performed using standard procedures using whole-cell lysates prepared in standard SDS sample buffer.

Chromosome spreads

Survivin stable cell lines (Fig. 3 A) and HeLa cells (Fig. 3 B) were treated with MG132 (10 µM) 10 h after release from single thymidine block (STB), and then collected 15 h after release to

prepare chromosome spreads. HeLa cells were treated with nocodazole (0.33 µM for Fig. 3 C; 3.3 µM for Fig. 3 D) 9 h after release from STB and then collected 12 h after release. To produce chromosome spreads, mitotic cells were obtained by selective detachment and then incubated in hypotonic buffer (75 mM KCl) at room temperature for 8–10 min. After attachment to glass coverslips by Cytospin at 1,500 rpm for 5 min, chromosome spreads were fixed with 2% PFA/PBS for 10 min, extracted with 0.5% Triton X-100/PBS for another 10 min, and then subjected to blocking with 3% BSA/PBS and subsequent immunostaining with primary antibodies for 2 h.

Fluorescence microscopy

Asynchronous U2OS-LacO cells were fixed with 2% PFA in PBS for 10 min and then extracted with 0.5% Triton X-100 for 5 min. For HeLa or HeLa-derived stable cell lines grown on coverslips, to stain Sgo1, H2ApT120, BubR1, Hec1, Hec1-pS44, and Knl1, cells were fixed with 2% PFA/PBS for 10 min and then extracted by 0.5% Triton X-100/PBS for 10 min; to stain Knl1-pS24, Knl1-pS60, and Knl1-pT180, cells were preextracted with 0.5% Triton X-100 in PHEM (60 mM Pipes, 25 mM Hepes, 10 mM EGTA, and 2 mM $MgCl_2$, pH 6.9) for 5 min and then fixed with 4% PFA in PHEM for 20 min. Fixed cells were stained with primary antibodies for 1–2 h and secondary antibodies for 1 h, all with 3% BSA in PBS with 0.1–0.5% Triton X-100 and at room temperature. DNA was stained for 10 min with DAPI. Fluorescence microscopy was performed at room temperature using a Nikon ECLIPSE Ni microscope with a Plan Apo Fluor 60× oil (NA 1.4) objective lens and a Clara charge-coupled devide (Andor Technology).

For K-fiber staining, cells were incubated with cold medium for 10 min. Then, after cells were extracted with 0.2% Triton X-100/PHEM for 1 min, an equal volume of 4% PFA/PHEM was added. After 5 min, the mixture was removed, and 4% PFA/PBS was added for 5 min. After blocking with 3% BSA/PBS, cells were stained with α-Tubulin antibody and ACA 1:1,000. Images were acquired through the entire cell as z stacks at 0.2-µm intervals on a deconvolution system (DeltaVision Elite Applied Precision/GE Healthcare) with a 100×/1.40-NA UPlanSApo objective (Olympus) using SoftWorx software (Applied Precision/GE Healthcare) and then deconvolved, and maximum-intensity projections were made using SoftWoRx.

Quantification of fluorescent intensity was performed with ImageJ (National Institutes of Health) using images obtained at identical illumination settings. Briefly, to quantify the relative intensity at the centromere/kinetochore, the average pixel intensity of H2ApT120, Sgo1, Bub1, Bub3, BubR1, Knl1, Knl1-pMELT, Knl1-pRVSF, Knl1-pSSILK, Hec1, Hec1-pS44, or ACA staining at centromeres/kinetochores, defined as a circular region encompassing at least three centromere pairs, was determined using ImageJ. After background correction, the ratio of centromere/kinetochore immunostaining intensity of these proteins versus that of ACA was calculated for each circular region. To quantify the means and SDs for the relative intensity of proteins of interest at centromeres/kinetochores from individual experiments, a total of 200 circular regions from 20 cells (10 nonoverlapping circular regions per cell) were plotted (Fig. 2, B, D, G, and I; Fig. S2, B, D, F, and H; Fig. S3 F; Fig. S4, B, D, and E; and Fig. S5, D–G). The means and SDs for the relative intensity of proteins of interest at centromeres/kinetochores from three independent experiments were quantified from 60 cells (20 cells per experiment), in which the average intensity of a single cell was determined by the means of 10 circular regions that contained >300 centromere pairs in total (Fig. 2, C, E, H, and J; Fig. 5, B, D, F, G, I, and J; Fig. 6, B, D, F, and G; Fig. 7, B, D, F, and G; Fig. 8, B and D; Fig. 9, B, C, E, and I; and Fig. S3, B and D).

To quantify the relative enrichment of proteins of interest at the LacO transgene array in U2OS-LacO cells (Fig. 1, B, C, E, and G), the average pixel intensity of H3pT3, H2ApT120, Aurora B, and Sgo1, within circles encompassing the EGFP-LacI fusion protein fluorescent signal at LacO transgene array and in the nearby nucleus, was determined. After background correction, the ratio of average immunostaining intensity at LacO repeats versus that in the nuclei was calculated. ImageJ was also used for the plot profiles of Aurora B, H2ApT120, and CENP-C at centromeres/kinetochores on chromosome spreads (Fig. 3, C and D). The intensities of Aurora B, H2ApT120, and CENP-C at centromeres/kinetochores were quantified along the lines of paired CENP-C dots. 10 sister centromeres were quantified and plotted for each cell. While the x axis represents the distance to the middle position of the paired CENP-C dots, the y axis represents the relative pixel intensities of Aurora B, H2ApT120, and CENP-C at the lines of CENP-C dots.

Time-lapse live cell imaging

Time-lapse live cell imaging was performed with the GE DV Elite Applied Precision DeltaVision system (GE Healthcare) equipped with Olympus oil objectives of 60× (NA 1.42) Plan Apo N or 40× (NA 1.35) UApo/340 and an API Custom Scientific complementary metal-oxide semiconductor camera, and Resolve3D softWoRx imaging software. Cells expressing H2B-GFP were plated in four-chamber glass-bottomed 35-mm dishes (Cellvis) coated with poly-D-lysine and filmed in a climate-controlled and humidified environment (37°C and 5% CO_2). Images were captured every 2 min. The acquired images were processed using Adobe Photoshop and Adobe Illustrator.

Statistical analysis

Statistical analyses were performed with a two-tailed unpaired Student's *t* test in GraphPad Prism 6. A P value of <0.05 was considered significant.

Online supplemental material

Fig. S1 shows the immunoblots demonstrating stable replacement of endogenous Survivin by exogenously expressed Survivin-Myc proteins and time-lapse live imaging of mitosis progression in HeLa or Survivin-Myc-expressing cells treated with DMSO, 5-ITu, and/or BAY 1816032, supporting Fig. 4. Fig. S2 shows that loss of the H3pT3–Survivin interaction hampers the removal of Bub3, Bub1, and BubR1 from metaphase kinetochores, supporting Fig. 5. Fig. S3 shows that loss of the H3pT3–Survivin interaction does not affect the kinetochore localization of Knl1 but hinders dephosphorylation of the Knl1-MELT motif at metaphase kinetochores, supporting Fig. 6. Fig. S4 shows that loss of the H3pT3–Survivin interaction impedes the dephosphorylation of the RVSF and SSILK motifs of Knl1 at metaphase kinetochores, supporting Fig. 7. Fig. S5

shows that tethering Sgo1 to the LacO array can recruit INCENP and Aurora B, and that loss of the H3pT3–Survivin interaction does not hamper the removal of Bub3 and Bub1 from metaphase kinetochores in cells expressing the H2ApT120 binding–deficient Sgo1-K492A mutant, supporting Fig. 8. Videos 1, 2, and 3 are related to Fig. 4 A and show time-lapse epifluorescence microscopy of mitosis progression in HeLa cells expressing Survivin-WT-Myc and H2B-GFP (Video 1), Survivin-K62A-Myc and H2B-GFP (Video 2), and Survivin-H80A-Myc and H2B-GFP (Video 3). Videos 4, 5, and 6 are related to Fig. 4 C and show time-lapse epifluorescence microscopy of mitosis progression in H2B-GFP–expressing HeLa cells treated with DMSO (Video 4) and H2B-GFP–expressing HeLa cells treated with 0.3 µM 5-ITu (Video 5) or 0.6 µM 5-ITu (Video 6). Videos 7 and 8 are related to Fig. 4 D and show time-lapse epifluorescence microscopy of mitosis progression in H2B-GFP–expressing HeLa cells released from MG132 into DMSO (Video 7) or 0.6 µM 5-ITu (Video 8). Videos 9 and 10 are related to Fig. S1 H and show time-lapse epifluorescence microscopy of mitosis progression in H2B-GFP–expressing HeLa cells treated with DMSO (Video 9) or 4 µM BAY 1816032 (Video 10).

Acknowledgments

We thank Drs. Xiangwei He and Jonathan Higgins for critically reading and commenting on the manuscript; Dr. Iain Cheeseman for discussion and suggestions; Drs. Iain Cheeseman, Jennifer DeLuca, Sabine Elowe, Hiroshi Kimura, Geert Kops, Jakob Nilsson, and David Spector for kindly providing reagents; and the Life Sciences Institute core facility for technical assistance.

This work was supported by grants to F. Wang from the National Key Research and Development Program of China (2017YFA0503600), the National Natural Science Foundation of China (31771499, 31571393, 31322032, 31371359, and 31561130155 to F. Wang; 81702552 to J. Xu), the Natural Science Foundation of Zhejiang Province (LZ19C070001), the Royal Society Newton Advanced Fellowship (NA140075), and the Fundamental Research Funds for the Central Universities in China (2014XZZX003-35 to F. Wang; 2019QNA7035 to J. Xu).

The authors declare no competing financial interests.

Author contributions: C. Liang and Z. Zhang designed and performed the majority of the experiments and analyzed the data, with contributions from Q. Chen, H. Yan, M. Zhang, L. Zhou, J. Xu, and W. Lu. F. Wang conceived the project, designed the experiments, analyzed the data, and wrote the manuscript.

Submitted: 13 July 2019
Revised: 14 November 2019
Accepted: 18 November 2019

References

Asghar, A., A. Lajeunesse, K. Dulla, G. Combes, P. Thebault, E.A. Nigg, and S. Elowe. 2015. Bub1 autophosphorylation feeds back to regulate kinetochore docking and promote localized substrate phosphorylation. *Nat. Commun.* 6:8364. https://doi.org/10.1038/ncomms9364

Banerjee, B., C.A. Kestner, and P.T. Stukenberg. 2014. EB1 enables spindle microtubules to regulate centromeric recruitment of Aurora B. *J. Cell Biol.* 204:947–963. https://doi.org/10.1083/jcb.201307119

Baron, A.P., C. von Schubert, F. Cubizolles, G. Siemeister, M. Hitchcock, A. Mengel, J. Schröder, A. Fernández-Montalván, F. von Nussbaum, D. Mumberg, and E.A. Nigg. 2016. Probing the catalytic functions of Bub1 kinase using the small molecule inhibitors BAY-320 and BAY-524. *eLife.* 5:e12187. https://doi.org/10.7554/eLife.12187

Bekier, M.E., T. Mazur, M.S. Rashid, and W.R. Taylor. 2015. Borealin dimerization mediates optimal CPC checkpoint function by enhancing localization to centromeres and kinetochores. *Nat. Commun.* 6:6775. https://doi.org/10.1038/ncomms7775

Biggins, S. 2013. The composition, functions, and regulation of the budding yeast kinetochore. *Genetics.* 194:817–846. https://doi.org/10.1534/genetics.112.145276

Caldas, G.V., and J.G. DeLuca. 2014. KNL1: bringing order to the kinetochore. *Chromosoma.* 123:169–181. https://doi.org/10.1007/s00412-013-0446-5

Caldas, G.V., K.F. DeLuca, and J.G. DeLuca. 2013. KNL1 facilitates phosphorylation of outer kinetochore proteins by promoting Aurora B kinase activity. *J. Cell Biol.* 203:957–969. https://doi.org/10.1083/jcb.201306054

Campbell, C.S., and A. Desai. 2013. Tension sensing by Aurora B kinase is independent of survivin-based centromere localization. *Nature.* 497:118–121. https://doi.org/10.1038/nature12057

Carmena, M., M. Wheelock, H. Funabiki, and W.C. Earnshaw. 2012. The chromosomal passenger complex (CPC): from easy rider to the godfather of mitosis. *Nat. Rev. Mol. Cell Biol.* 13:789–803. https://doi.org/10.1038/nrm3474

Cheeseman, I.M. 2014. The kinetochore. *Cold Spring Harb. Perspect. Biol.* 6:a015826. https://doi.org/10.1101/cshperspect.a015826

Cheeseman, I.M., J.S. Chappie, E.M. Wilson-Kubalek, and A. Desai. 2006. The conserved KMN network constitutes the core microtubule-binding site of the kinetochore. *Cell.* 127:983–997. https://doi.org/10.1016/j.cell.2006.09.039

Ciferri, C., J. De Luca, S. Monzani, K.J. Ferrari, D. Ristic, C. Wyman, H. Stark, J. Kilmartin, E.D. Salmon, and A. Musacchio. 2005. Architecture of the human ndc80-hec1 complex, a critical constituent of the outer kinetochore. *J. Biol. Chem.* 280:29088–29095. https://doi.org/10.1074/jbc.M504070200

Ciferri, C., S. Pasqualato, E. Screpanti, G. Varetti, S. Santaguida, G. Dos Reis, A. Maiolica, J. Polka, J.G. De Luca, P. De Wulf, et al. 2008. Implications for kinetochore-microtubule attachment from the structure of an engineered Ndc80 complex. *Cell.* 133:427–439. https://doi.org/10.1016/j.cell.2008.03.020

Cimini, D., X. Wan, C.B. Hirel, and E.D. Salmon. 2006. Aurora kinase promotes turnover of kinetochore microtubules to reduce chromosome segregation errors. *Curr. Biol.* 16:1711–1718. https://doi.org/10.1016/j.cub.2006.07.022

Dai, J., S. Sultan, S.S. Taylor, and J.M. Higgins. 2005. The kinase haspin is required for mitotic histone H3 Thr 3 phosphorylation and normal metaphase chromosome alignment. *Genes Dev.* 19:472–488. https://doi.org/10.1101/gad.1267105

Dai, J., B.A. Sullivan, and J.M. Higgins. 2006. Regulation of mitotic chromosome cohesion by Haspin and Aurora B. *Dev. Cell.* 11:741–750. https://doi.org/10.1016/j.devcel.2006.09.018

De Antoni, A., S. Maffini, S. Knapp, A. Musacchio, and S. Santaguida. 2012. A small-molecule inhibitor of Haspin alters the kinetochore functions of Aurora B. *J. Cell Biol.* 199:269–284. https://doi.org/10.1083/jcb.201205119

DeLuca, J.G., W.E. Gall, C. Ciferri, D. Cimini, A. Musacchio, and E.D. Salmon. 2006. Kinetochore microtubule dynamics and attachment stability are regulated by Hec1. *Cell.* 127:969–982. https://doi.org/10.1016/j.cell.2006.09.047

DeLuca, K.F., S.M. Lens, and J.G. DeLuca. 2011. Temporal changes in Hec1 phosphorylation control kinetochore-microtubule attachment stability during mitosis. *J. Cell Sci.* 124:622–634. https://doi.org/10.1242/jcs.072629

DeLuca, K.F., A. Meppelink, A.J. Broad, J.E. Mick, O.B. Peersen, S. Pektas, S.M.A. Lens, and J.G. DeLuca. 2018. Aurora A kinase phosphorylates Hec1 to regulate metaphase kinetochore-microtubule dynamics. *J. Cell Biol.* 217:163–177. https://doi.org/10.1083/jcb.201707160

Du, J., A.E. Kelly, H. Funabiki, and D.J. Patel. 2012. Structural basis for recognition of H3T3ph and Smac/DIABLO N-terminal peptides by human Survivin. *Structure.* 20:185–195. https://doi.org/10.1016/j.str.2011.12.001

Espert, A., P. Uluocak, R.N. Bastos, D. Mangat, P. Graab, and U. Gruneberg. 2014. PP2A-B56 opposes Mps1 phosphorylation of Knl1 and thereby promotes spindle assembly checkpoint silencing. *J. Cell Biol.* 206:833–842. https://doi.org/10.1083/jcb.201406109

Espeut, J., D.K. Cheerambathur, L. Krenning, K. Oegema, and A. Desai. 2012. Microtubule binding by KNL-1 contributes to spindle checkpoint silencing at the kinetochore. *J. Cell Biol.* 196:469–482. https://doi.org/10.1083/jcb.201111107

Fink, S., K. Turnbull, A. Desai, and C.S. Campbell. 2017. An engineered minimal chromosomal passenger complex reveals a role for INCENP/Sli15 spindle association in chromosome biorientation. *J. Cell Biol.* 216: 911–923. https://doi.org/10.1083/jcb.201609123

Fischböck-Halwachs, J., S. Singh, M. Potocnjak, G. Hagemann, V. Solis-Mezarino, S. Woike, M. Ghodgaonkar-Steger, F. Weissmann, L.D. Gallego, J. Rojas, et al. 2019. The COMA complex interacts with Cse4 and positions Sli15/Ipl1 at the budding yeast inner kinetochore. *eLife.* 8:e42879. https://doi.org/10.7554/eLife.42879

Garcia-Rodriguez, L.J., T. Kasciukovic, V. Denninger, and T.U. Tanaka. 2019. Aurora B-INCENP Localization at Centromeres/Inner Kinetochores Is Required for Chromosome Bi-orientation in Budding Yeast. *Curr. Biol.* 29:1536–1544.

Gregan, J., S. Polakova, L. Zhang, I.M. Tolić-Nørrelykke, and D. Cimini. 2011. Merotelic kinetochore attachment: causes and effects. *Trends Cell Biol.* 21:374–381. https://doi.org/10.1016/j.tcb.2011.01.003

Guimaraes, G.J., Y. Dong, B.F. McEwen, and J.G. Deluca. 2008. Kinetochore-microtubule attachment relies on the disordered N-terminal tail domain of Hec1. *Curr. Biol.* 18:1778–1784. https://doi.org/10.1016/j.cub.2008.08.012

Haase, J., M.K. Bonner, H. Halas, and A.E. Kelly. 2017. Distinct Roles of the Chromosomal Passenger Complex in the Detection of and Response to Errors in Kinetochore-Microtubule Attachment. *Dev. Cell.* 42: 640–654.e645.

Hauf, S., R.W. Cole, S. LaTerra, C. Zimmer, G. Schnapp, R. Walter, A. Heckel, J. van Meel, C.L. Rieder, and J.M. Peters. 2003. The small molecule Hesperadin reveals a role for Aurora B in correcting kinetochore-microtubule attachment and in maintaining the spindle assembly checkpoint. *J. Cell Biol.* 161:281–294. https://doi.org/10.1083/jcb.200208092

Hendrickx, A., M. Beullens, H. Ceulemans, T. Den Abt, A. Van Eynde, E. Nicolaescu, B. Lesage, and M. Bollen. 2009. Docking motif-guided mapping of the interactome of protein phosphatase-1. *Chem. Biol.* 16: 365–371. https://doi.org/10.1016/j.chembiol.2009.02.012

Hengeveld, R.C.C., M.J.M. Vromans, M. Vleugel, M.A. Hadders, and S.M.A. Lens. 2017. Inner centromere localization of the CPC maintains centromere cohesion and allows mitotic checkpoint silencing. *Nat. Commun.* 8:15542. https://doi.org/10.1038/ncomms15542

Hindriksen, S., S.M.A. Lens, and M.A. Hadders. 2017. The Ins and Outs of Aurora B Inner Centromere Localization. *Front. Cell Dev. Biol.* 5:112. https://doi.org/10.3389/fcell.2017.00112

Janicki, S.M., T. Tsukamoto, S.E. Salghetti, W.P. Tansey, R. Sachidanandam, K.V. Prasanth, T. Ried, Y. Shav-Tal, E. Bertrand, R.H. Singer, and D.L. Spector. 2004. From silencing to gene expression: real-time analysis in single cells. *Cell.* 116:683–698. https://doi.org/10.1016/S0092-8674(04)00171-0

Jeyaprakash, A.A., C. Basquin, U. Jayachandran, and E. Conti. 2011. Structural basis for the recognition of phosphorylated histone h3 by the survivin subunit of the chromosomal passenger complex. *Structure.* 19: 1625–1634. https://doi.org/10.1016/j.str.2011.09.002

Kawashima, S.A., Y. Yamagishi, T. Honda, K. Ishiguro, and Y. Watanabe. 2010. Phosphorylation of H2A by Bub1 prevents chromosomal instability through localizing shugoshin. *Science.* 327:172–177. https://doi.org/10.1126/science.1180189

Kelly, A.E., C. Ghenoiu, J.Z. Xue, C. Zierhut, H. Kimura, and H. Funabiki. 2010. Survivin reads phosphorylated histone H3 threonine 3 to activate the mitotic kinase Aurora B. *Science.* 330:235–239. https://doi.org/10.1126/science.1189505

Knowlton, A.L., W. Lan, and P.T. Stukenberg. 2006. Aurora B is enriched at merotelic attachment sites, where it regulates MCAK. *Curr. Biol.* 16: 1705–1710. https://doi.org/10.1016/j.cub.2006.07.057

Krenn, V., and A. Musacchio. 2015. The Aurora B Kinase in Chromosome Bi-Orientation and Spindle Checkpoint Signaling. *Front. Oncol.* 5:225. https://doi.org/10.3389/fonc.2015.00225

Krenn, V., K. Overlack, I. Primorac, S. van Gerwen, and A. Musacchio. 2014. KI motifs of human Knl1 enhance assembly of comprehensive spindle checkpoint complexes around MELT repeats. *Curr. Biol.* 24:29–39. https://doi.org/10.1016/j.cub.2013.11.046

Lampson, M.A., and I.M. Cheeseman. 2011. Sensing centromere tension: Aurora B and the regulation of kinetochore function. *Trends Cell Biol.* 21: 133–140. https://doi.org/10.1016/j.tcb.2010.10.007

Lampson, M.A., K. Renduchitala, A. Khodjakov, and T.M. Kapoor. 2004. Correcting improper chromosome-spindle attachments during cell division. *Nat. Cell Biol.* 6:232–237. https://doi.org/10.1038/ncb1102

Lan, W., X. Zhang, S.L. Kline-Smith, S.E. Rosasco, G.A. Barrett-Wilt, J. Shabanowitz, D.F. Hunt, C.E. Walczak, and P.T. Stukenberg. 2004. Aurora B phosphorylates centromeric MCAK and regulates its localization and microtubule depolymerization activity. *Curr. Biol.* 14:273–286. https://doi.org/10.1016/j.cub.2004.01.055

Liang, C., Q. Chen, Q. Yi, M. Zhang, H. Yan, B. Zhang, L. Zhou, Z. Zhang, F. Qi, S. Ye, and F. Wang. 2018. A kinase-dependent role for Haspin in antagonizing Wapl and protecting mitotic centromere cohesion. *EMBO Rep.* 19:43–56. https://doi.org/10.15252/embr.201744737

Liang, C., Z. Zhang, Q. Chen, H. Yan, M. Zhang, X. Xiang, Q. Yi, X. Pan, H. Cheng, and F. Wang. 2019. A positive feedback mechanism ensures proper assembly of the functional inner centromere during mitosis in human cells. *J. Biol. Chem.* 294:1437–1450. https://doi.org/10.1074/jbc.RA118.006046

Liu, D., G. Vader, M.J. Vromans, M.A. Lampson, and S.M. Lens. 2009. Sensing chromosome bi-orientation by spatial separation of aurora B kinase from kinetochore substrates. *Science.* 323:1350–1353. https://doi.org/10.1126/science.1167000

Liu, D., M. Vleugel, C.B. Backer, T. Hori, T. Fukagawa, I.M. Cheeseman, and M.A. Lampson. 2010. Regulated targeting of protein phosphatase 1 to the outer kinetochore by KNL1 opposes Aurora B kinase. *J. Cell Biol.* 188: 809–820. https://doi.org/10.1083/jcb.201001006

Liu, H., L. Jia, and H. Yu. 2013. Phospho-H2A and cohesin specify distinct tension-regulated Sgo1 pools at kinetochores and inner centromeres. *Curr. Biol.* 23:1927–1933. https://doi.org/10.1016/j.cub.2013.07.078

Liu, H., Q. Qu, R. Warrington, A. Rice, N. Cheng, and H. Yu. 2015. Mitotic Transcription Installs Sgo1 at Centromeres to Coordinate Chromosome Segregation. *Mol. Cell.* 59:426–436. https://doi.org/10.1016/j.molcel.2015.06.018

London, N., and S. Biggins. 2014. Signalling dynamics in the spindle checkpoint response. *Nat. Rev. Mol. Cell Biol.* 15:736–747. https://doi.org/10.1038/nrm3888

London, N., S. Ceto, J.A. Ranish, and S. Biggins. 2012. Phosphoregulation of Spc105 by Mps1 and PP1 regulates Bub1 localization to kinetochores. *Curr. Biol.* 22:900–906. https://doi.org/10.1016/j.cub.2012.03.052

Meadows, J.C., L.A. Shepperd, V. Vanoosthuyse, T.C. Lancaster, A.M. Sochaj, G.J. Buttrick, K.G. Hardwick, and J.B. Millar. 2011. Spindle checkpoint silencing requires association of PP1 to both Spc7 and kinesin-8 motors. *Dev. Cell.* 20:739–750. https://doi.org/10.1016/j.devcel.2011.05.008

Miller, S.A., M.L. Johnson, and P.T. Stukenberg. 2008. Kinetochore attachments require an interaction between unstructured tails on microtubules and Ndc80(Hec1). *Curr. Biol.* 18:1785–1791. https://doi.org/10.1016/j.cub.2008.11.007

Monda, J.K., and I.M. Cheeseman. 2018. The kinetochore-microtubule interface at a glance. *J. Cell Sci.* 131:jcs214577. https://doi.org/10.1242/jcs.214577

Musacchio, A. 2015. The Molecular Biology of Spindle Assembly Checkpoint Signaling Dynamics. *Curr. Biol.* 25:R1002–R1018. https://doi.org/10.1016/j.cub.2015.08.051

Musacchio, A., and A. Desai. 2017. A Molecular View of Kinetochore Assembly and Function. *Biology (Basel).* 6:E5. https://doi.org/10.3390/biology6010005

Niedzialkowska, E., F. Wang, P.J. Porebski, W. Minor, J.M. Higgins, and P.T. Stukenberg. 2012. Molecular basis for phosphospecific recognition of histone H3 tails by Survivin paralogues at inner centromeres. *Mol. Biol. Cell.* 23:1457–1466. https://doi.org/10.1091/mbc.e11-11-0904

Nijenhuis, W., G. Vallardi, A. Teixeira, G.J. Kops, and A.T. Saurin. 2014. Negative feedback at kinetochores underlies a responsive spindle checkpoint signal. *Nat. Cell Biol.* 16:1257–1264. https://doi.org/10.1038/ncb3065

Pachis, S.T., Y. Hiruma, E.C. Tromer, A. Perrakis, and G. Kops. 2019. Interactions between N-terminal Modules in MPS1 Enable Spindle Checkpoint Silencing. *Cell Reports.* 26:2101–2112.e2106.

Pinsky, B.A., C.R. Nelson, and S. Biggins. 2009. Protein phosphatase 1 regulates exit from the spindle checkpoint in budding yeast. *Curr. Biol.* 19: 1182–1187. https://doi.org/10.1016/j.cub.2009.06.043

Primorac, I., J.R. Weir, E. Chiroli, F. Gross, I. Hoffmann, S. van Gerwen, A. Ciliberto, and A. Musacchio. 2013. Bub3 reads phosphorylated MELT repeats to promote spindle assembly checkpoint signaling. *eLife.* 2: e01030. https://doi.org/10.7554/eLife.01030

Rosenberg, J.S., F.R. Cross, and H. Funabiki. 2011. KNL1/Spc105 recruits PP1 to silence the spindle assembly checkpoint. *Curr. Biol.* 21:942–947. https://doi.org/10.1016/j.cub.2011.04.011

Samejima, K., M. Platani, M. Wolny, H. Ogawa, G. Vargiu, P.J. Knight, M. Peckham, and W.C. Earnshaw. 2015. The Inner Centromere Protein (INCENP) Coil Is a Single α-Helix (SAH) Domain That Binds Directly to Microtubules and Is Important for Chromosome Passenger Complex (CPC) Localization and Function in Mitosis. *J. Biol. Chem.* 290: 21460–21472. https://doi.org/10.1074/jbc.M115.645317

Shepperd, L.A., J.C. Meadows, A.M. Sochaj, T.C. Lancaster, J. Zou, G.J. Buttrick, J. Rappsilber, K.G. Hardwick, and J.B. Millar. 2012. Phosphodependent recruitment of Bub1 and Bub3 to Spc7/KNL1 by Mph1 kinase maintains the spindle checkpoint. *Curr. Biol.* 22:891–899. https://doi.org/10.1016/j.cub.2012.03.051

Siemeister, G., A. Mengel, A.E. Fernández-Montalván, W. Bone, J. Schröder, S. Zitzmann-Kolbe, H. Briem, S. Prechtl, S.J. Holton, U. Mönning, et al. 2019. Inhibition of BUB1 Kinase by BAY 1816032 Sensitizes Tumor Cells toward Taxanes, ATR, and PARP Inhibitors *In Vitro* and *In Vivo*. *Clin. Cancer Res.* 25:1404–1414. https://doi.org/10.1158/1078-0432.CCR-18-0628

Tanaka, T.U., N. Rachidi, C. Janke, G. Pereira, M. Galova, E. Schiebel, M.J. Stark, and K. Nasmyth. 2002. Evidence that the Ipl1-Sli15 (Aurora kinase-INCENP) complex promotes chromosome bi-orientation by altering kinetochore-spindle pole connections. *Cell.* 108:317–329. https://doi.org/10.1016/S0092-8674(02)00633-5

Tang, Z., H. Shu, W. Qi, N.A. Mahmood, M.C. Mumby, and H. Yu. 2006. PP2A is required for centromeric localization of Sgo1 and proper chromosome segregation. *Dev. Cell.* 10:575–585. https://doi.org/10.1016/j.devcel.2006.03.010

Thompson, S.L., S.F. Bakhoum, and D.A. Compton. 2010. Mechanisms of chromosomal instability. *Curr. Biol.* 20:R285–R295. https://doi.org/10.1016/j.cub.2010.01.034

Trivedi, P., and P.T. Stukenberg. 2016. A Centromere-Signaling Network Underlies the Coordination among Mitotic Events. *Trends Biochem. Sci.* 41:160–174. https://doi.org/10.1016/j.tibs.2015.11.002

Tsukahara, T., Y. Tanno, and Y. Watanabe. 2010. Phosphorylation of the CPC by Cdk1 promotes chromosome bi-orientation. *Nature.* 467:719–723. https://doi.org/10.1038/nature09390

van der Horst, A., M.J. Vromans, K. Bouwman, M.S. van der Waal, M.A. Hadders, and S.M. Lens. 2015. Inter-domain Cooperation in INCENP Promotes Aurora B Relocation from Centromeres to Microtubules. *Cell Reports.* 12:380–387. https://doi.org/10.1016/j.celrep.2015.06.038

Vanoosthuyse, V., and K.G. Hardwick. 2009. A novel protein phosphatase 1-dependent spindle checkpoint silencing mechanism. *Curr. Biol.* 19:1176–1181. https://doi.org/10.1016/j.cub.2009.05.060

Varma, D., and E.D. Salmon. 2012. The KMN protein network--chief conductors of the kinetochore orchestra. *J. Cell Sci.* 125:5927–5936. https://doi.org/10.1242/jcs.093724

Vleugel, M., M. Omerzu, V. Groenewold, M.A. Hadders, S.M.A. Lens, and G.J.P.L. Kops. 2015. Sequential multisite phospho-regulation of KNL1-BUB3 interfaces at mitotic kinetochores. *Mol. Cell.* 57:824–835. https://doi.org/10.1016/j.molcel.2014.12.036

Vleugel, M., E. Tromer, M. Omerzu, V. Groenewold, W. Nijenhuis, B. Snel, and G.J. Kops. 2013. Arrayed BUB recruitment modules in the kinetochore scaffold KNL1 promote accurate chromosome segregation. *J. Cell Biol.* 203:943–955. https://doi.org/10.1083/jcb.201307016

Wan, X., R.P. O'Quinn, H.L. Pierce, A.P. Joglekar, W.E. Gall, J.G. DeLuca, C.W. Carroll, S.T. Liu, T.J. Yen, B.F. McEwen, et al. 2009. Protein architecture of the human kinetochore microtubule attachment site. *Cell.* 137:672–684. https://doi.org/10.1016/j.cell.2009.03.035

Wang, F., J. Dai, J.R. Daum, E. Niedzialkowska, B. Banerjee, P.T. Stukenberg, G.J. Gorbsky, and J.M. Higgins. 2010. Histone H3 Thr-3 phosphorylation by Haspin positions Aurora B at centromeres in mitosis. *Science.* 330:231–235. https://doi.org/10.1126/science.1189435

Wang, F., N.P. Ulyanova, J.R. Daum, D. Patnaik, A.V. Kateneva, G.J. Gorbsky, and J.M. Higgins. 2012. Haspin inhibitors reveal centromeric functions of Aurora B in chromosome segregation. *J. Cell Biol.* 199:251–268. https://doi.org/10.1083/jcb.201205106

Welburn, J.P., M. Vleugel, D. Liu, J.R. Yates III, M.A. Lampson, T. Fukagawa, and I.M. Cheeseman. 2010. Aurora B phosphorylates spatially distinct targets to differentially regulate the kinetochore-microtubule interface. *Mol. Cell.* 38:383–392. https://doi.org/10.1016/j.molcel.2010.02.034

Wheelock, M.S., D.J. Wynne, B.S. Tseng, and H. Funabiki. 2017. Dual recognition of chromatin and microtubules by INCENP is important for mitotic progression. *J. Cell Biol.* 216:925–941. https://doi.org/10.1083/jcb.201609061

Yamagishi, Y., T. Honda, Y. Tanno, and Y. Watanabe. 2010. Two histone marks establish the inner centromere and chromosome bi-orientation. *Science.* 330:239–243. https://doi.org/10.1126/science.1194498

Yamagishi, Y., C.H. Yang, Y. Tanno, and Y. Watanabe. 2012. MPS1/Mph1 phosphorylates the kinetochore protein KNL1/Spc7 to recruit SAC components. *Nat. Cell Biol.* 14:746–752. https://doi.org/10.1038/ncb2515

Yoo, T.Y., J.M. Choi, W. Conway, C.H. Yu, R.V. Pappu, and D.J. Needleman. 2018. Measuring NDC80 binding reveals the molecular basis of tension-dependent kinetochore-microtubule attachments. *eLife.* 7:e36392. https://doi.org/10.7554/eLife.36392

Yue, Z., A. Carvalho, Z. Xu, X. Yuan, S. Cardinale, S. Ribeiro, F. Lai, H. Ogawa, E. Gudmundsdottir, R. Gassmann, et al. 2008. Deconstructing Survivin: comprehensive genetic analysis of Survivin function by conditional knockout in a vertebrate cell line. *J. Cell Biol.* 183:279–296. https://doi.org/10.1083/jcb.200806118

Zhang, G., T. Lischetti, and J. Nilsson. 2014. A minimal number of MELT repeats supports all the functions of KNL1 in chromosome segregation. *J. Cell Sci.* 127:871–884. https://doi.org/10.1242/jcs.139725

Zhou, L., C. Liang, Q. Chen, Z. Zhang, B. Zhang, H. Yan, F. Qi, M. Zhang, Q. Yi, Y. Guan, et al. 2017. The N-Terminal Non-Kinase-Domain-Mediated Binding of Haspin to Pds5B Protects Centromeric Cohesion in Mitosis. *Curr. Biol.* 27:992–1004. https://doi.org/10.1016/j.cub.2017.02.019